Roles of putative Rho-GEF Gef2 in division-site positioning and contractile-ring function in fission yeast cytokinesis

Yanfang Ye[a,b], I-Ju Lee[a,c], Kurt W. Runge[d], and Jian-Qiu Wu[a,b]
[a]Department of Molecular Genetics, [b]Department of Molecular and Cellular Biochemistry, and [c]Graduate Program of Molecular, Cellular, and Developmental Biology, The Ohio State University, Columbus, OH 43210; [d]Department of Molecular Genetics, Cleveland Clinic Lerner College of Medicine, Cleveland, OH 44195

ABSTRACT Cytokinesis is crucial for integrating genome inheritance and cell functions. In multicellular organisms, Rho-guanine nucleotide exchange factors (GEFs) and Rho GTPases are key regulators of division-plane specification and contractile-ring formation during cytokinesis, but how they regulate early steps of cytokinesis in fission yeast remains largely unknown. Here we show that putative Rho-GEF Gef2 and Polo kinase Plo1 coordinate to control the medial cortical localization and function of anillin-related protein Mid1. The division-site positioning defects of *gef2Δ plo1-ts18* double mutant can be partially rescued by increasing Mid1 levels. We find that Gef2 physically interacts with the Mid1 N-terminus and modulates Mid1 cortical binding. Gef2 localization to cortical nodes and the contractile ring depends on its last 145 residues, and the DBL-homology domain is important for its function in cytokinesis. Our data suggest the interaction between Rho-GEFs and anillins is an important step in the signaling pathways during cytokinesis. In addition, Gef2 also regulates contractile-ring function late in cytokinesis and may negatively regulate the septation initiation network. Collectively, we propose that Gef2 facilitates and stabilizes Mid1 binding to the medial cortex, where the localized Mid1 specifies the division site and induces contractile-ring assembly.

Monitoring Editor
Rong Li
Stowers Institute

Received: Sep 21, 2011
Revised: Jan 13, 2012
Accepted: Jan 26, 2012

INTRODUCTION

Cytokinesis, the last stage of the cell cycle, partitions a mother cell into two daughter cells. Cytokinesis requires coordination of four key events: division-plane selection, contractile-ring assembly, constriction and disassembly of the contractile ring, and plasma membrane fusion and daughter-cell separation (Balasubramanian *et al.*, 2004; Barr and Gruneberg, 2007; Pollard and Wu, 2010). The last step involves septum formation in fungi and midbody formation in animal cells. To ensure that daughter cells faithfully inherit chromosomes from mother cells, cytokinesis must be tightly spatiotemporally controlled and coordinated with mitosis (Storchova and Pellman, 2004). Cytokinesis failure leads to genomic instability and tumorigenesis (Fujiwara *et al.*, 2005; Sagona and Stenmark, 2010).

In animal cells signals from the central spindle/spindle midzone, astral microtubules, or both are required to ensure that cytokinetic events occur properly on the cell cortex (Bringmann and Hyman, 2005; Cabernard *et al.*, 2010). Many studies have shown that the Polo kinase/Rho-guanine nucleotide exchange factor (GEF)/Rho GTPase module regulates the signaling from the central spindle to the cortex to trigger contractile-ring assembly and cytokinesis (Petronczki *et al.*, 2008). At anaphase, the conserved Polo kinase promotes the complex formation of Cyk-4/MgcRacGAP/RacGAP50C, a subunit of the centralspindlin complex, and Ect2/Pebble, a Rho-GEF (Petronczki *et al.*, 2007; Wolfe *et al.*, 2009). Binding of Ect2 to Cyk-4 recruits Ect2 to the division site (Somers and Saint, 2003; Yüce *et al.*, 2005; Zhao and Fang, 2005; Nishimura

This article was published online ahead of print in MBoC in Press (http://www.molbiolcell.org/cgi/doi/10.1091/mbc.E11-09-0800) on February 1, 2012.

Address correspondence to: Jian-Qiu Wu (wu.620@osu.edu).

Abbreviations used: aa, amino acids; DH, DBL-homology; DIC, differential interference contrast; FL, full length; FRAP, fluorescence recovery after photobleaching; GEF, guanine nucleotide exchange factor; IP, immunoprecipitation; Lat-A, latrunculin A; mECitrine, monomeric enhanced Citrine; mEGFP, monomeric enhanced green fluorescent protein; mYFP, monomeric yellow fluorescent protein; NLS, nuclear localization sequence; PH, pleckstrin homology; ROI, region of interest; SIN, septation initiation network; SPB, spindle pole body; tdTomato, tandem Tomato; wt, wild type.

© 2012 Ye *et al.* This article is distributed by The American Society for Cell Biology under license from the author(s). Two months after publication it is available to the public under an Attribution–Noncommercial–Share Alike 3.0 Unported Creative Commons License (http://creativecommons.org/licenses/by-nc-sa/3.0).
"ASCB®," "The American Society for Cell Biology®," and "Molecular Biology of the Cell®" are registered trademarks of The American Society of Cell Biology.

and Yonemura, 2006). This determines the cleavage plane by locally activating GTPase RhoA, which in turn recruits and activates downstream effectors, such as anillin, nonmuscle myosin-II, and actin nucleator formin, eventually leading to contractile-ring formation and cleavage-furrow ingression (Hall, 1998; Shandala *et al.*, 2004; Gregory *et al.*, 2008; Hickson and O'Farrell, 2008; Piekny and Glotzer, 2008; Piekny and Maddox, 2010). The Polo/GEF/Rho module is also conserved in the budding yeast *Saccharomyces cerevisiae*, in which Polo kinase Cdc5 phosphorylates and recruits Rho-GEF Tus1 to the bud neck (Yoshida *et al.*, 2006). The Rho-GEF promotes Rho1 recruitment and activation and consequently induces actomyosin-ring formation and cytokinesis (Tolliday *et al.*, 2002; Yoshida *et al.*, 2006).

Cells of the fission yeast *Schizosaccharomyces pombe* are rod shaped and divide by medial fission. The anillin-like protein Mid1 and its regulators Polo kinase Plo1 and DYRK kinase Pom1 specify the division site in fission yeast (Almonacid and Paoletti, 2010). During interphase, Mid1 shuttles between the nucleus and interphase nodes on the plasma membrane near the nucleus (Sohrmann *et al.*, 1996; Bähler *et al.*, 1998a; Paoletti and Chang, 2000). Nodes refer to discrete protein clusters (20–65) on the equatorial plasma membrane (Wu *et al.*, 2006; Laporte *et al.*, 2010, 2011). Pom1 kinase forms a polar gradient on the plasma membrane and confines Mid1 to the cell middle through Cdr2 kinase (Celton-Morizur *et al.*, 2006; Padte *et al.*, 2006; Huang *et al.*, 2007; Almonacid *et al.*, 2009; Martin and Berthelot-Grosjean, 2009; Moseley *et al.*, 2009; Hachet *et al.*, 2011). Cdr2 establishes interphase nodes by recruiting Cdr1 kinase, Mid1, Blt1, Rho-GEF Gef2, kinesin-like protein Klp8, and Wee1 kinase (Breeding *et al.*, 1998; Morrell *et al.*, 2004; Martin and Berthelot-Grosjean, 2009; Moseley *et al.*, 2009). The Pom1 gradient and interphase nodes coordinate to regulate cell size and mitotic entry (Martin and Berthelot-Grosjean, 2009; Moseley *et al.*, 2009; Hachet *et al.*, 2011). Besides Cdr2's role in recruiting Mid1 by binding to its N-terminus (Almonacid *et al.*, 2009), functions of other interphase-node proteins in cytokinesis are unknown. At G2/M transition, Mid1 is phosphorylated by Plo1 at multiple sites and completely exits from the nucleus to form cytokinesis nodes at cell equator (Bähler *et al.*, 1998a; Paoletti and Chang, 2000; Almonacid *et al.*, 2011).

Mid1 in cytokinesis nodes recruits essential contractile-ring components, IQGAP Rng2, myosin-II (heavy chain Myo2 and light chains Cdc4 and Rlc1), F-BAR protein Cdc15, and the formin Cdc12 to form mature cytokinesis nodes, the precursors of the contractile ring (Wu *et al.*, 2003, 2006; Almonacid *et al.*, 2011; Laporte *et al.*, 2011; Padmanabhan *et al.*, 2011). Cdc12 nucleates the majority of actin filaments for contractile-ring formation (Kovar *et al.*, 2003; Coffman *et al.*, 2009). The nodes condense into a compact contractile ring by interactions between actin filaments and myosin-II through a search, capture, pull, and release mechanism at early mitosis (Bähler *et al.*, 1998a; Wu *et al.*, 2006; Vavylonis *et al.*, 2008; Coffman *et al.*, 2009; Laporte *et al.*, 2011; Ojkic *et al.*, 2011). The ring matures by increasing Cdc15 concentration and by recruiting other components during anaphase B under the regulation of the septation initiation network (SIN) pathway (Wu *et al.*, 2003; Wu and Pollard, 2005; Hachet and Simanis, 2008; Huang *et al.*, 2008). At the onset of ring constriction after spindle breakdown, Mid1 disappears from the contractile ring and returns to the nucleus and then to interphase nodes (Paoletti and Chang, 2000; Wu *et al.*, 2003). Although Mid1 is essential for division-site positioning and cytokinesis-node formation, it is not essential for contractile-ring formation. Without Mid1, the Plo1-activated SIN pathway is required for ring assembly (Hachet and Simanis, 2008; Huang *et al.*, 2008), although this pathway is involved in ring maturation in *mid1*$^{+}$ cells (Wu *et al.*, 2003). While the Mid1-independent pathway is capable of ring formation, it is far less efficient than the Mid1-dependent pathway and cannot position the division plane correctly. Plo1 is involved in both pathways for ring assembly, suggesting that Plo1 is a key regulator in cytokinesis. However, whether Rho-GEFs and Rho GTPases regulate division-site selection and contractile-ring assembly in *S. pombe* remains largely unknown.

S. pombe contains six Rho GTPases (Cdc42 and Rho1–5) and seven Rho GEFs (Scd1, Gef1–3, and Rgf1–3). Cdc42 mainly controls cell polarity, and Scd1 and Gef1 induce its activation (Coll *et al.*, 2003; Hirota *et al.*, 2003). Rho1 is a regulatory subunit of (1,3)-β-D-glucan synthase and regulates cell wall/septum formation, as well as cell polarization. Rho1 is activated by Rgf1–3 (Tajadura *et al.*, 2004; Morrell-Falvey *et al.*, 2005; Mutoh *et al.*, 2005; Garcia *et al.*, 2006, 2009a, 2009b; Wu *et al.*, 2010). Rho2 and Rho5 are also involved in cell wall/septum formation (Calonge *et al.*, 2000; Nakano *et al.*, 2005). Rho3 modulates exocytosis and cell polarity (Nakano *et al.*, 2002; Wang *et al.*, 2003). Rho4 regulates septum degradation (Santos *et al.*, 2005). Although Rgf3 might be involved in contractile-ring assembly (Mutoh *et al.*, 2005), no Rho-GEFs and Rho GTPases have been shown to play a role in division-site positioning. The functions of Gef2 and Gef3 are unknown, but the localization of Gef2 in cortical nodes and the contractile ring implies that Gef2 might play a role in early cytokinesis (Iwaki *et al.*, 2003; Moseley *et al.*, 2009).

In this study, we find that putative Rho-GEF Gef2 is involved in division-site and contractile-ring positioning by interacting with anillin-related protein Mid1. This function overlaps with that of Polo kinase Plo1. In addition, Gef2 also stabilizes the contractile ring during its constriction. Thus the Rho-GEF does have a function in early stages of cytokinesis in fission yeast.

RESULTS

Putative Rho-GEF Gef2 and Polo kinase Plo1 coordinate to regulate division-site and contractile-ring positioning

We hypothesized that functional redundancy is responsible for the lack of obvious phenotypes of Rho-GEF mutants in early stages of cytokinesis (see *Introduction*). To elucidate this overlapping function, synthetic interactions between Rho-GEF mutants (*rgf1Δ, rgf2Δ, 81nmt1-rgf3*, *gef1Δ*, and *gef2Δ*) and mutations that affect early stages of cytokinesis were investigated. We found that *gef2Δ* had synthetic negative interactions with *plo1, mid1, cdc4-8, rng2-D5,* and *myo2-E1* mutants. Among these interactions, *gef2Δ* showed strongest synthetic defects with *plo1-ts18* and *mid1* mutants, which were chosen for further studies.

gef2Δ cells resembled wild-type (wt) cells with a septum at the cell center and perpendicular to the cell long axis during cytokinesis, as reported (Iwaki *et al.*, 2003). In this study, we defined a septum formed within the central 20% of the cell as a normal septum (Figure 1, A and B). At 25°C, 7% cells with abnormal septa were observed (Figure 1, A and B) in *plo1-ts18* mutant, which has a mutation in the kinase domain and severe defects in division-site positioning and contractile-ring assembly at 36°C (MacIver *et al.*, 2003). In contrast, ~95% *gef2Δ plo1-ts18* double-mutant cells formed abnormal septa at 25°C, many septa were aberrant or even parallel to the cell long axis (Figure 1, A and B). Similar results were observed in the double mutants of *gef2Δ* and other *plo1* temperature-sensitive alleles at 32°C (Supplemental Figure S1).

Because septum formation is guided by the contractile ring, we wondered whether the contractile ring was also defective in *gef2Δ plo1-ts18* mutant. Myosin-II heavy chain Myo2 and light chain Rlc1, F-BAR protein Cdc15, and actin filament marker green fluorescent

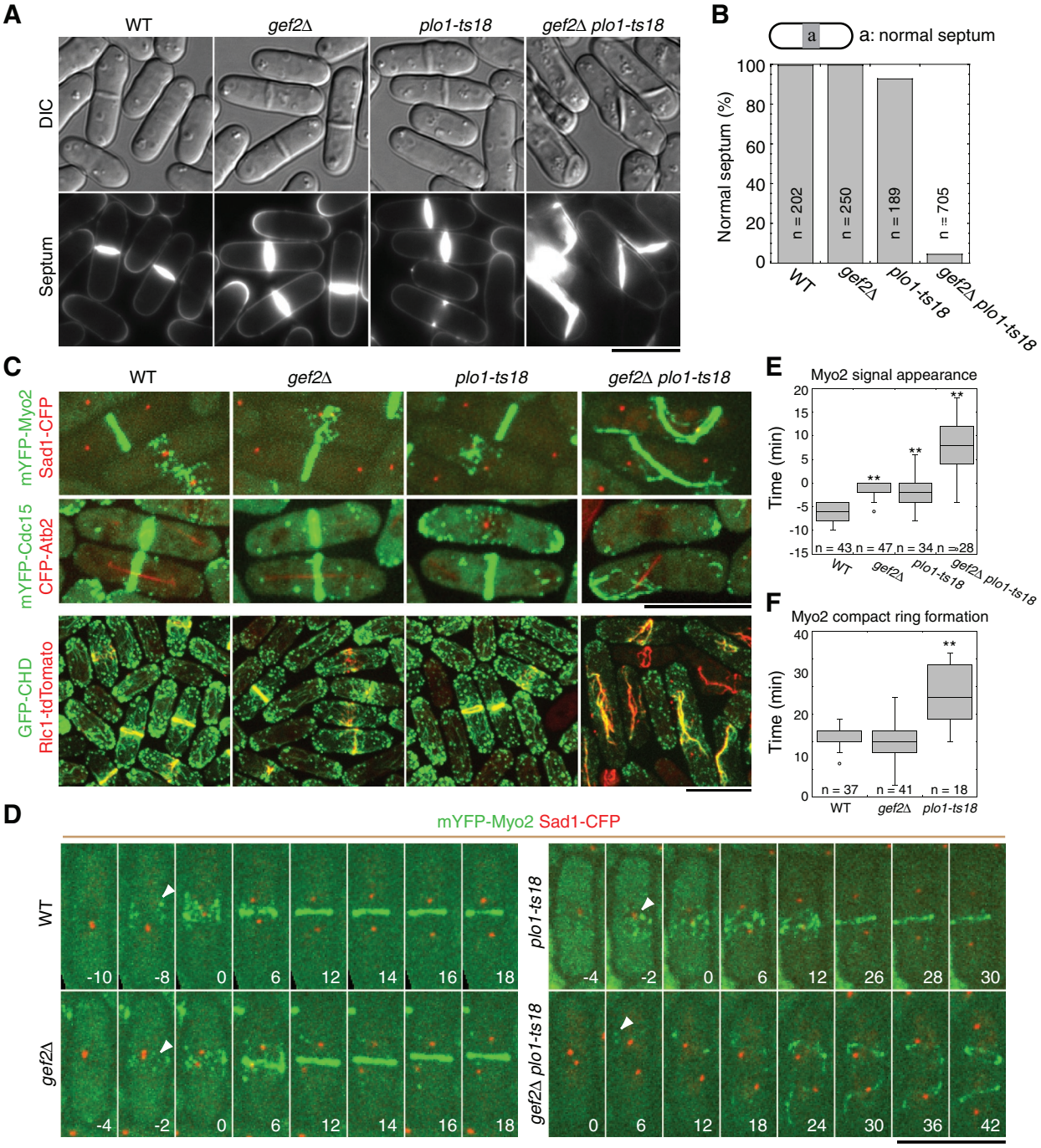

FIGURE 1: Putative Rho-GEF Gef2 is required for division-site positioning and contractile-ring assembly when Polo kinase Plo1 function is compromised. Cells were grown and examined at 25°C. (A) Septum-positioning defects of *gef2Δ plo1-ts18* mutant. Top, differential interference contrast (DIC). Bottom, calcofluor staining of the same cells. Strains used were wt (JW2556; see Supplemental Table S1), *gef2Δ* (JW3184), *plo1-ts18* (JW3079), and *gef2Δ plo1-ts18* (JW3078). (B) Quantification of septum positioning in calcofluor-stained cells as in A. In this and other figures, we defined a septum formed within the central 20% of the cell as a normal septum. (C) Defects in contractile-ring assembly and positioning in *gef2Δ plo1-ts18* cells. Ring formation was examined in wt, *gef2Δ*, *plo1-ts18*, and *gef2Δ plo1-ts18* cells expressing mYFP-Myo2 Sad1-CFP (JW3547, JW3546, JW3066, and JW3067), mYFP-Cdc15 CFP-Atb2 (JW3186, JW3185, JW3076, and JW3077), and GFP-CHD Rlc1-tdTomato (JW3554, JW3555, JW3230, and JW3229). GFP-CHD expression was induced for 21 h in EMM5S medium without thiamine. (D–F) Time courses (in minutes) of ring formation in wt (JW3547), *gef2Δ* (JW3546), *plo1-ts18* (JW3066), and *gef2Δ plo1-ts18* (JW3067) cells expressing mYFP-Myo2 and Sad1-CFP. (D, E) Time 0 is the time of SPB separation. (D) Arrowheads indicate the appearance of mYFP-Myo2 nodes or signal (in *gef2Δ plo1-ts18* cells). Images are maximum-intensity projections of seven z-projections at 0.75-μm spacing. (E) Timing of mYFP-Myo2 signal appearance in cytokinesis nodes at the cell equator or a random location (for *gef2Δ plo1-ts18* cells only). (F) Duration of mYFP-Myo2 compact ring (without lagging nodes) formation from the appearance of nodes. Because *gef2Δ plo1-ts18* cells did not form rings during the movie or had severe delay in the formation of misplaced rings, no quantification is shown. $^{**}p < 0.01$. Bars, 10 μm.

protein–calponin homology domain of IQGAP Rng2 (GFP-CHD; Wachtler *et al.*, 2003; Karagiannis *et al.*, 2005; Martin and Chang, 2006) were used to observe ring formation, and spindle pole body (SPB) protein Sad1 and α-tubulin Atb2 (Sato *et al.*, 2009) were used to monitor cell-cycle stages (Figure 1, C–F). All wt and *gef2Δ* cells and majority of *plo1-ts18* cells formed cytokinesis nodes at G2/M transition and contractile rings before anaphase B at the cell equator (Figure 1, C and D, and Supplemental Videos S1–S3). Consistent with previous studies (Wu *et al.*, 2003, 2006; Laporte *et al.*, 2011), Myo2 appeared as a broad band of precursor nodes 5.9 ± 1.8 min before SPB separation in wt cells, which condensed into a compact ring without lagging nodes 20.2 ± 2.1 min after its appearance (Figure 1, D–F). Both *gef2Δ* and *plo1-ts18* mutants showed a small but significant delay in Myo2 node recruitment, which appeared at 1.6 ± 1.5 min ($p < 0.001$) and 2.1 ± 3.2 min ($p < 0.001$) before SPB separation, respectively. The compact-ring formation took 19.3 ± 3.4 min ($p = 0.16$) in *gef2Δ* and 28.0 ± 5.4 min ($p < 0.001$) in *plo1-ts18* (Figure 1, D–F). In contrast, no nodes were detected in *gef2Δ plo1-ts18* cells (Figure 1, C and D). Myo2 signal appeared at random location ~7.3 ± 7.0 min ($p < 0.001$ compared with wt) after SPB separation and then formed aberrant filaments (Figure 1E). Some of the filaments could eventually form a misplaced contractile ring after a long delay (Figure 1, C and D, and Supplemental Video S4), but many cells failed to assemble the ring. Similar results were obtained in time-lapse movies using strains expressing monomeric yellow fluorescent protein (mYFP)–Cdc15 and CFP-Atb2. *plo1-ts18* cells were defective in mitotic spindle (Figure 1, C and D, and unpublished data). However, from 19 to 32°C, *gef2Δ* had no obvious synthetic interaction with cold-sensitive β-tubulin mutant *nda3-KM311*, which blocks the spindle formation at the restrictive temperature (Hiraoka *et al.*, 1984). Thus the synthetic phenotype of *gef2Δ plo1-ts18* cells is not caused by defective spindle. Together, Gef2 is involved in division-site positioning and contractile-ring assembly, but these roles are masked by the dominant functions of Polo kinase Plo1.

Several proteins, including Blt1 and kinesin-like protein Klp8, also localize to interphase nodes similar to Gef2 (Moseley *et al.*, 2009). We wondered whether these proteins are required for division-site positioning in the sensitized *plo1*-mutant background. *plo1-ts18* had no obvious synthetic defects in septum positioning with *klp8Δ*. Nine percent of *blt1Δ plo1-ts18* (n = 273 septating cells) and 55% of *cdr2Δ plo1-ts18* (n = 231) cells displayed abnormal septa at 25°C. In addition, unlike *cdr2Δ*, *gef2Δ* cells showed small defects in cell-size control since its length at septation was 14.6 ± 0.9 μm (n = 100 cells) compared with 13.7 ± 0.9 μm of wt cells (n = 105) and ~20 μm of *cdr2Δ* cells (Martin and Berthelot-Grosjean, 2009; Moseley *et al.*, 2009). Therefore Gef2 and to a lesser degree Cdr2, but not Blt1 or Klp8, are critical for division-site specification in the *plo1*-mutant background.

Mid1 localization and dynamics are regulated by both Gef2 and Plo1

The defects in division-site positioning and contractile-ring formation of *gef2Δ plo1-ts18* mutant were reminiscent of the *mid1*-mutant phenotypes (Chang *et al.*, 1996; Sohrmann *et al.*, 1996; Bähler *et al.*, 1998a; Paoletti and Chang, 2000). To explore the molecular mechanism of the defects in *gef2Δ plo1-ts18* mutant, we examined Mid1-monomeric enhanced GFP (mEGFP) or Mid1-monomeric enhanced Citrine (mECitrine; a YFP variant) localization and dynamics in wt, *gef2Δ*, *plo1-ts18*, and *gef2Δ plo1-ts18* mutants with or without the Cdr2 kinase (Figure 2, A–E). The defects did not seem to be caused by Mid1 protein levels because Mid1 global concentrations in these mutants were not dramatically different from that in wt cells (Figure 2C and Supplemental Figure S2). During interphase, Mid1 localized to the nucleus and interphase nodes in the three mutants, similar in distribution and intensity to those of wt (Figure 2, A and C, and unpublished data).

At G2/M transition, nuclear Mid1 disappeared, whereas the cortical Mid1 nodes increased in intensity and coalesced into a ring in wt and *gef2Δ* cells (Figure 2, A, B, and D, and Supplemental Video S5). Plo1 phosphorylates Mid1 and regulates its nuclear export (Bähler *et al.*, 1998a; Almonacid *et al.*, 2011). *plo1-ts18* cells were defective in Mid1 nuclear export, but they still formed cytokinesis nodes and contractile ring at cell center at 25°C, although the Mid1 concentration in the nodes was reduced twofold compared to those in wt and *gef2Δ* cells (Figure 2, A and D, and Supplemental Videos S5 and S6). As expected, in *gef2Δ* and *plo1-ts18* single mutants, myosin-II light-chain Rlc1 colocalized with Mid1 at nodes and the contractile ring at the cell equator during early mitosis (Figure 2A and Supplemental Video S5). However, no Mid1 and Rlc1 colocalization was observed in *gef2Δ plo1-ts18* cells. Mid1 nodes failed to condense into a compact ring during mitosis, whereas Rlc1 appeared randomly in the cytoplasm and then formed aberrant filamentous structures or tilted ring (Figure 2A and Supplemental Video S5). In *cdr2Δ gef2Δ plo1-ts18* cells, Mid1 remained in the nucleus (with similar concentration to *plo1-ts18* cells) and cytoplasm, the Mid1 ring was abolished, and Mid1 concentration in cytokinesis nodes was only ~10% of that in wt (Figure 2, B and D, and Supplemental Video S7), indicating that the cortical nodes in *gef2Δ plo1-ts18* cells are mainly Cdr2-dependent interphase nodes. Thus the division-site positioning and contractile-ring formation defects of *gef2Δ plo1-ts18* cells could be due to the failure of Mid1 recruitment to the plasma membrane at G2/M transition.

Next we tested whether Gef2 regulates Mid1 dynamics and stability on the plasma membrane, using fluorescence recovery after photobleaching (FRAP). Mid1 in interphase nodes was more dynamic in *gef2Δ*, with a half-time of recovery 97 ± 71 s, compared with 184 ± 100 s in wt (Figure 2E; $p = 0.04$). Although the dynamics of Mid1 in cytokinesis nodes was not significantly affected in *gef2Δ* cells (Figure 2E; $p = 0.68$), the mobile fraction of Mid1 in *gef2Δ*, 40 ± 15%, was significantly higher than that in wt, 29 ± 14% (Figure 2E; $p = 0.04$). Moreover, immunoprecipitation (IP) of fission yeast extracts revealed that Mid1 interacted with Gef2; deletion of Cdr2 reduced but did not block the interaction (Figure 2F). Together these results suggest that Gef2 might modulate Mid1 cortical binding by physical interactions.

Mid1 overexpression or artificial targeting of Mid1 to cortical nodes partially rescues *gef2Δ plo1-ts18* defects in division-site positioning

We hypothesized that both Gef2 and Plo1 regulate Mid1 localization to cortical nodes, Plo1 phosphorylates Mid1 to promote its nuclear export (Bähler *et al.*, 1998a; Almonacid *et al.*, 2011), and Gef2 facilitates and stabilizes Mid1 cortical anchoring. In *gef2Δ plo1-ts18* cells, the additive defects reduce Mid1 level in cortical nodes (Figure 2, B and D) and result in failures to recruit downstream ring components to the cell equator. If so, increasing Mid1 expression or Mid1 concentration in nodes was predicted to suppress the defects in *gef2Δ plo1-ts18* cells. We created *gef2Δ plo1-ts18* strains containing either an extra copy of the *mid1*$^+$ gene (Celton-Morizur *et al.*, 2004) or endogenous *mid1*$^+$ under the control of inducible *urg1* promoter (Watt *et al.*, 2008). As expected, both two *mid1*$^+$ copies and *Purg1* induced Mid1 overexpression partially rescued the septum-positioning defects of *gef2Δ plo1-ts18*

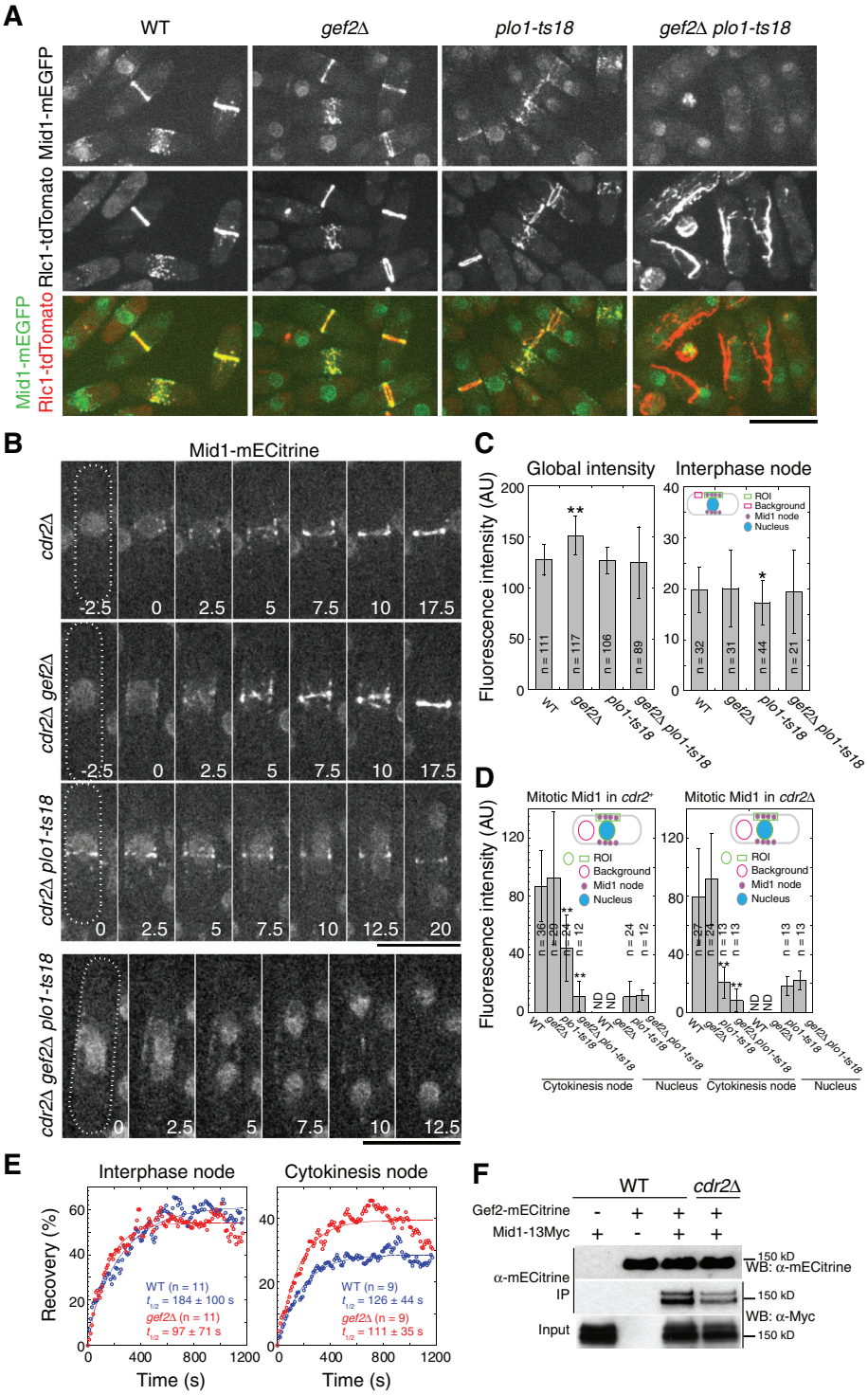

FIGURE 2: Gef2 is important for anillin Mid1 localization and dynamics. (A) Mid1 cannot form a ring in *gef2Δ plo1-ts18*. Mid1 localization in the indicated strains JW4231-JW4234 expressing Mid1-mEGFP and Rlc1-tdTomato at 25°C. (B) Time courses (in minutes) of Mid1-mECitrine (a YFP variant) ring formation in the indicated *cdr2Δ* strains JW3578, JW3575, JW3577, and JW3576. Images are maximum-intensity projections of three z-projections at 1.2-µm spacing. Time 0 in *cdr2Δ* and *cdr2Δ gef2Δ* cells marks the appearance of Mid1 cytokinesis nodes and in *cdr2Δ plo1-ts18* and *cdr2Δ gef2Δ plo1-ts18* cells is the start of the movies. Bars, 10 µm. (C) Mid1 concentrations in whole cells and in interphase nodes. Left, the cell-size-corrected fluorescence intensity in whole cells (mean ± SD) is the intensity of Mid1-mECitrine–expressing strain subtracting the intensity of the corresponding strain without Mid1-mECitrine. From left to right: intensity of JW3323 – JW2556, JW3324 – JW3184, JW3559 – JW3079, and JW3558 – JW3078. Right, mean fluorescence intensity (mean ± SD) of interphase Mid1-mECitrine nodes measured as described in *Materials and Methods*. Strains (left to right): JW3323, JW3324, JW3559, and JW3558. *0.01 < p < 0.05 and **p < 0.01 compared with wt. (D) Mid1 concentrations in cytokinesis nodes and the nucleus during early mitosis. Mean fluorescence intensity (mean ± SD) of Mid1-mECitrine in the indicated strains in *cdr2*⁺ and *cdr2Δ* backgrounds. Strains were the same as in B and C. **p < 0.01 compared with wt. In early mitotic cells of wt and *gef2Δ*, Mid1 nuclear signal is very close to the cytoplasmic background and therefore not determined (ND). (E) Mid1 cortical nodes are more dynamic or mobile in *gef2Δ* mutant. FRAP curves of Mid1-mECitirne in wt (JW3323) and *gef2Δ* (JW3324) cells. (F) Gef2 coIP with Mid1. Antibody against mECitrine was used in IP. IPs were carried out from cell extracts of *mid1-13Myc* (JW3254), *gef2-mECitrine* (JW2997), *mid1-13Myc gef2-mECitrine* (JW3255), and *cdr2Δ mid1-13Myc gef2-mECitrine* (JW3333).

mutant, and normal septum positioning was restored to 30 and 50% from ~8%, respectively (Figure 3A). Consistently, mitotic *gef2Δ plo1-ts18* cells (with mitotic spindle) containing the Mid1 ring increased from <3 to 24% when two copies of Mid1 were expressed (Figure 3B).

Furthermore, we tested whether artificially targeting Mid1 to medial cortical nodes rescues the defects of *gef2Δ plo1-ts18*. We fused Cdr2-mEGFP to the C-terminus of Mid1 under native *mid1* promoter and integrated it at the *mid1* locus. The fusion protein localized to the medial cortical nodes as expected, and the signal was much stronger than wt Mid1 at nodes but much weaker in the nucleus in *gef2Δ plo1-ts18* cells (Figure 3C). Of interest, Mid1-Cdr2-mEGFP also partially rescued the defects of *gef2Δ plo1-ts18* mutant; 17% of cells displayed normal septum positioning (Figure 3C). Collectively, these results suggest that the defect in *gef2Δ plo1-ts18* mutant is indeed caused by the lack of sufficient functional Mid1 in cortical nodes (see *Discussion*).

Gef2 interacts with Mid1 N-terminus and is essential for its cortical localization

It is known that Mid1 is targeted to the plasma membrane using two independent mechanisms: one involves an amphipathic helix and the adjacent polybasic nuclear localization sequence (NLS) at its C-terminus; the other involves the interaction between Mid1(400-450) and Cdr2 kinase (Celton-Morizur *et al.*, 2004; Almonacid *et al.*, 2009). To further dissect how Gef2 regulates Mid1 localization and function, we investigated genetic interactions between *gef2Δ* and

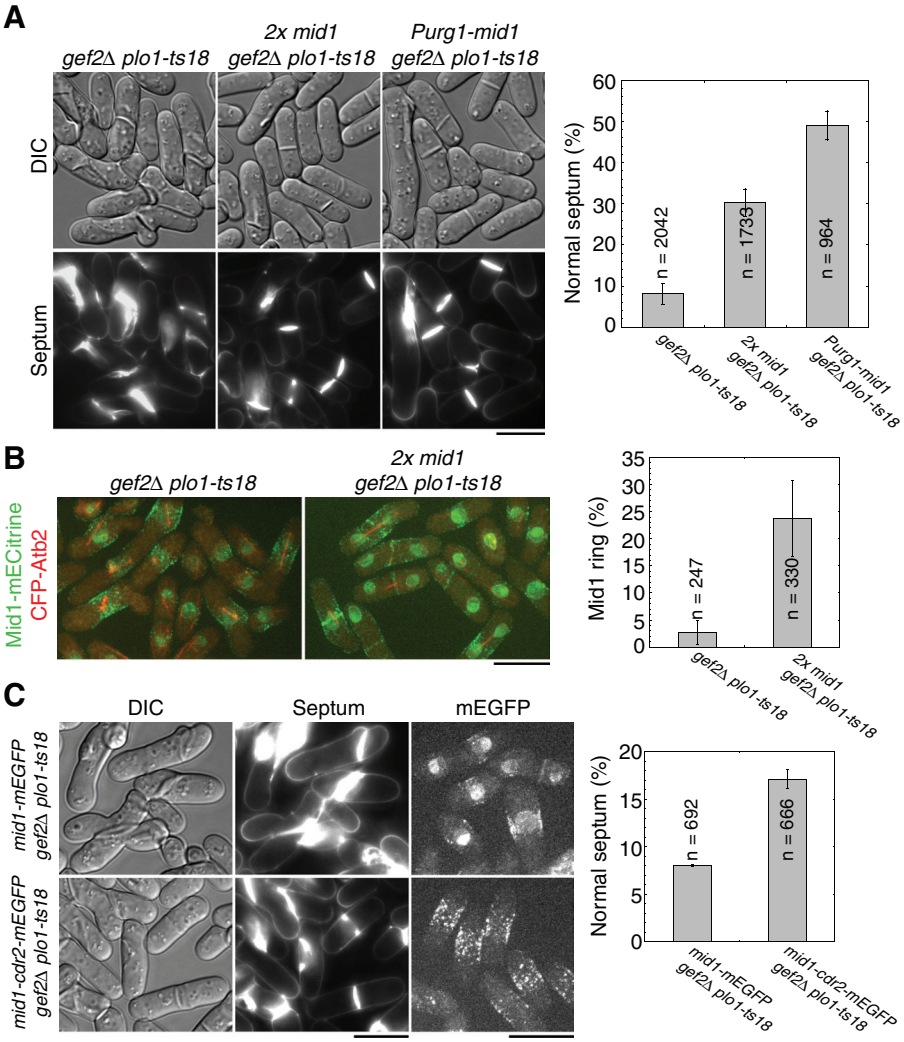

FIGURE 3: Overexpression of Mid1 rescues *gef2Δ plo1-ts18* defects in division-site positioning. (A) Overexpression of Mid1 under different promoters partially rescues septum-positioning defect in *gef2Δ plo1-ts18* cells. *gef2Δ plo1-ts18* (JW3078), *2x mid1 gef2Δ plo1-ts18* (an extra copy *Pmid1-mid1* integrated at the *leu1* locus in addition to the native *mid1*; JW3242), and *gef2Δ plo1-ts18 Purg1-mid1* (integrated at the *mid1* locus and induced in media with uracil; JW3237) were grown in YE5S medium at 25°C for 24 h. Top, DIC; bottom, calcofluor staining. Septum positioning in calcofluor-stained cells was quantified (right). Mean ± SD from three independent experiments. (B) Two copies of Mid1 partially rescue Mid1 ring formation in *gef2Δ plo1-ts18* cells expressing Mid1-mECitrine and CFP-Atb2. Strains JW3281 and JW3383 grown at 25°C. The percentage of mitotic cells (with a spindle) with a Mid1 ring was quantified from two experiments. (C) Mid1-Cdr2 fusion protein partially rescues septum-positioning defect in *gef2Δ plo1-ts18* cells. Left, DIC; middle, calcofluor staining; right, Mid1-mEGFP (top, JW3560) or Mid1-Cdr2-mEGFP (bottom, JW3426). Septum positioning in calcofluor-stained cells was quantified from two experiments. Bars, 10 µm.

mid1 mutants/truncations (Figure 4, Supplemental Figure S3, and unpublished data). Strong synthetic defects in septum positioning were observed in double mutants of *gef2Δ* and *81nmt1-mECitrine-mid1* (under repressing condition), *mid1-6, mid1-366, mid1(1-580)*, and *mid1(1-506)* (Figure 4, A and B, and Supplemental Figure S3, A and B). In addition, severe synthetic defects in septum positioning were observed in a double mutant of *gef2Δ* and the *mid1(Helix*)* mutant, which has mutations in the C-terminal amphipathic helix and severely affects Mid1 cortical binding (Celton-Morizur *et al.*, 2004), but the defects were not observed in a double mutant of *gef2Δ* and the *mid1(NLS*)* mutant, which impairs Mid1 nuclear localization but is dispensable for Mid1 cortical localization (Celton-Morizur *et al.*, 2004; Figure 4, A and B). These interactions suggest that Gef2 may regulate Mid1 function through its N-terminus.

Consistent with previous studies (Celton-Morizur *et al.*, 2004; Lee and Wu, 2012), Mid1(1-506) and Mid1(1-580) localized to cytoplasm, nucleus, faint cortex nodes, and the contractile ring (Figure 4, C–E). However, their node and ring localizations were abolished in *gef2Δ* cells, whereas misplaced Rlc1 ring or filaments but not cytokinesis nodes were still present (Figure 4, C and D). The loss of Mid1 localization to the contractile ring or filaments was Cdr2 independent (Figure 4E). In contrast, the localization of Mid1 C-terminal fragment Mid1(507-920) did not require Gef2 (Supplemental Figure S3C). Consistent with the localization dependence, an interaction was detected between Gef2 and Mid1(1-506) but not between Gef2 and Mid1(507-920) in IP (Figure 4F). Thus Gef2 interacts with Mid1 N-terminus and is essential for its cortical localization.

We further tested the Mid1 domain/motif required for the interaction with Gef2. Mid1(300-350) and Mid1(400-450) are important for Mid1(1-506) localization and function (Almonacid *et al.*, 2009). We hypothesized that these regions might bind to Gef2. Indeed, IP using yeast extracts revealed that the interaction between Gef2 and Mid1 was severely weakened in *mid1(Δ300-350)* strain and to a lesser degree in *mid1(Δ400-450)* strain (Figure 4G). Because Mid1(400-450) but not Mid1(300-350) binds to Cdr2 kinase (Almonacid *et al.*, 2009) and Cdr2 also affects the interaction between Gef2 and full-length (FL) Mid1 (Figure 2F), it is likely that Mid1(300-350) binds to Gef2. Consistently, *mid1(Δ300-350) plo1-ts18* double mutant resembled *gef2Δ plo1-ts18* cells with severe defects in septum positioning (Figure 4H). Together these results suggest that Gef2 physically interacts with Mid1 through Mid1(300-350) to regulate Mid1's cortical localization and stability, and this interaction is Cdr2 independent.

Dependence of Gef2 localization on Blt1 but not on actin filaments

We next investigated Gef2 localization. As reported (Moseley *et al.*, 2009), Gef2 localizes to interphase nodes, cytokinesis nodes, and the contractile ring (Figure 5A). Compared to Mid1 (Wu and Pollard, 2005; Laporte *et al.*, 2011), each average cell had 4270 ± 1190 Gef2 molecules and each interphase node contained 14 ± 6 Gef2 molecules (Figure 5B). An interphase node has 17 Mid1 molecules (Laporte *et al.*, 2011), suggesting that Mid1 and Gef2 may bind to each other stoichiometrically during interphase. FRAP analysis revealed that the half-time of recovery of interphase Gef2 node was 115 ± 42 s (Figure 5C), which suggests

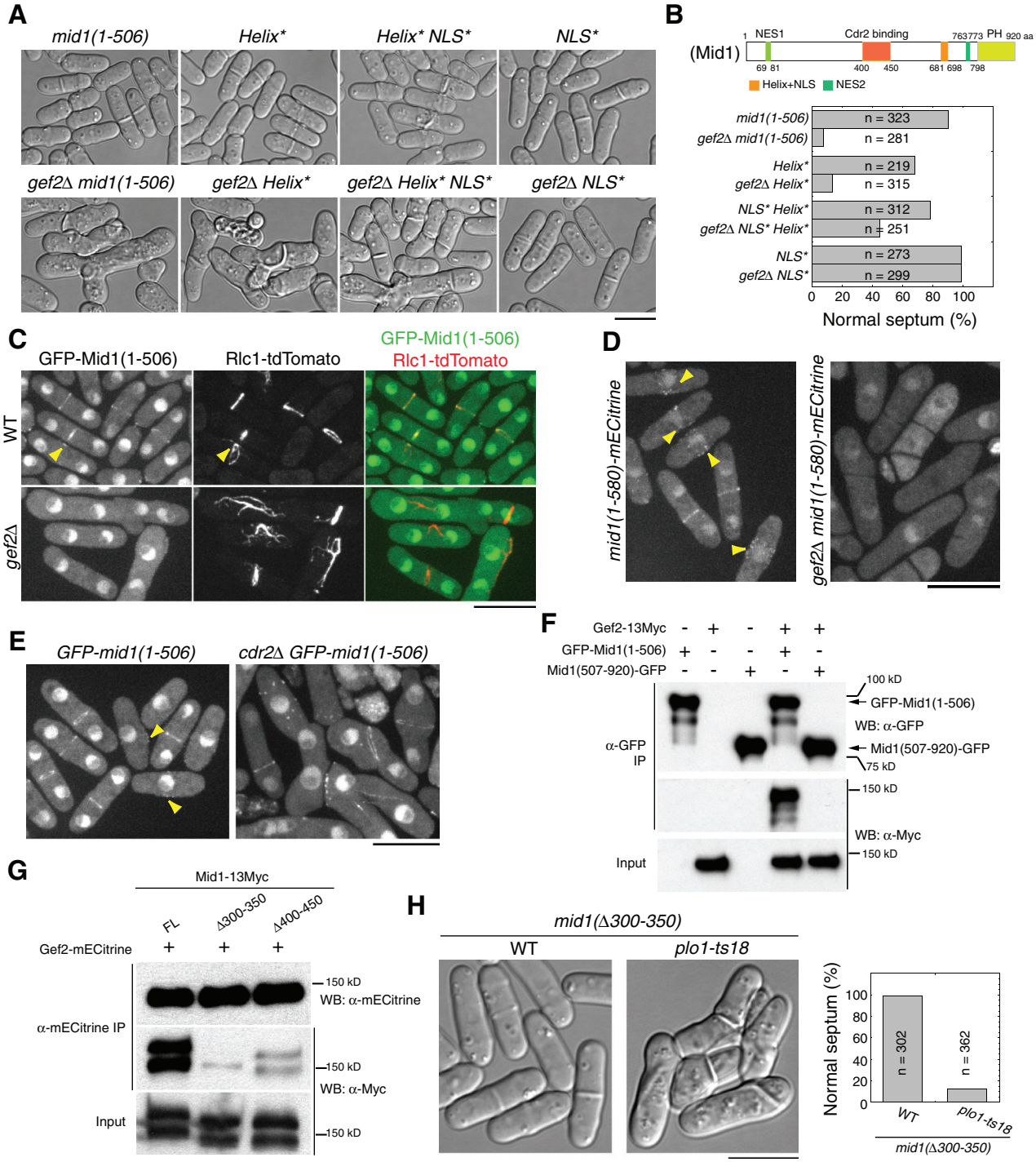

FIGURE 4: Gef2 interacts with Mid1 N-terminus and is essential for its cortical localization. (A, B) Gef2 is required for division-site positioning when Mid1 cortical localization is compromised. (A) DIC images and (B) quantification of septum positioning at 25°C in *mid1* and *gef2Δ mid1* mutants AP998, AP583, AP630, AP734, JW3570, JW3567, JW3721, and JW3568. Schematic of Mid1 domains is shown in B. (C) Mid1(1-506) cortical localization is abolished in *gef2Δ*. Cells expressing GFP-Mid1(1-506) and Rlc1-tdTomato in *gef2*$^+$ (JW3628) and *gef2Δ* (JW3629) were grown at 25°C. Arrowheads indicate signals at early mitosis. (D) Mid1(1-580)-mECitrine localizations to cortical nodes and the contractile ring depend on Gef2. JW2603 and JW3670 cells at 25°C. Arrowheads indicate cortical nodes. (E) Mid1(1-506) still localizes to the contractile ring in *cdr2Δ* cells. AP998 and JW3647 cells at 25°C. Arrowheads indicate cortical nodes. (F) Gef2 coIP with Mid1(1-506) but not Mid1(507-920). IP using antibody against GFP was carried out in cell extracts of *GFP-mid1(1-506)* (AP998), *gef2-13Myc* (JW3204), *mid1(507-920)-GFP* (AP621), *gef2-13Myc GFP-mid1(1-506)* (JW3623), and *gef2-13Myc mid1(507-920)-GFP* (JW3624). (G) The interaction between Gef2 and Mid1 is significantly weakened in *mid1* mutants lacking the cortical-targeting domains. IP using antibody against mECitrine was carried out in cell extracts of *gef2-mECitrine mid1-13Myc* (JW3255), *gef2-mECitrine mid1(Δ300-350)-13Myc* (JW3829), and *gef2-mECitrine mid1(Δ400-450)-13Myc* (JW3830). (H) DIC and quantification of septum-positioning defects in *plo1-ts18 mid1(Δ300-350)*. Strains of AP1977 and JW3705 grown at 25°C. Bars, 10 μm.

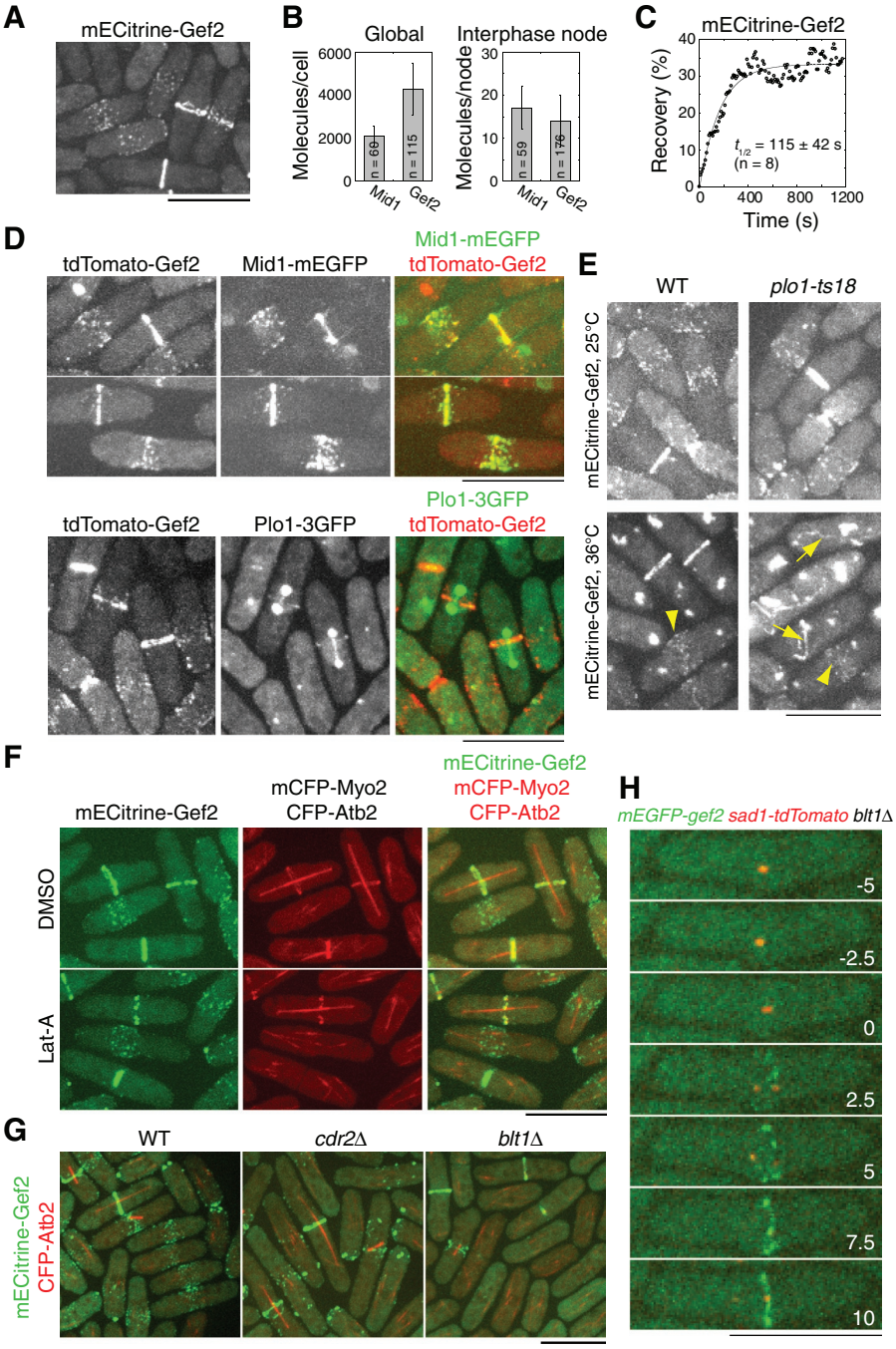

FIGURE 5: Dependence of Gef2 localization on Blt1 during interphase but not during mitosis. (A) mECitrine-Gef2 (JW3825) localizes to cortical nodes and the contractile ring. (B) Counting Gef2 globally in the whole cells and in interphase nodes. Molecule numbers of Gef2 (JW3825) were normalized to those of Mid1. (C) FRAP analysis of Gef2 (JW3825). Cells were bleached at time zero, and images were taken with 10 s delay. (D) Colocalization of Gef2 with Mid1 and Plo1. Cells expressing tdTomato-Gef2 Mid1-mEGFP (JW4236; top) and tdTomato-Gef2 Plo1-3GFP (JW4235; bottom) were grown at 25°C. (E) Plo1 is not required for Gef2 localization. Cells expressing mECitrine-Gef2 (JW3825 and JW3843) were grown at 25°C and then shifted to 36°C for 2 h. Arrows indicate aberrant filaments; arrowheads indicate nodes. (F) Actin filaments are not required for Gef2 node and ring localizations. Cells expressing mECitrine-Gef2 mCFP-Myo2 CFP-Atb2 (JW3853) were treated with dimethyl sulfoxide or 100 μM Lat-A for 5 min at 25°C. (G) Gef2 interphase-node localization but not cytokinesis-node and contractile-ring localization depends on Cdr2 kinase and Blt1. wt (JW3852), *cdr2Δ* (JW3846), and *blt1Δ* (JW3848) cells expressing mECitrine-Gef2 CFP-Atb2 were grown at 25°C. (H) Time course (in minutes) of mEGFP-Gef2 localization to cytokinesis nodes and the contractile ring in *blt1Δ* cells (JW4237). Time 0 indicates SPB separation. Images are maximum-intensity projections of four z-projections at 1.2 μm spacing. Bars, 10 μm.

that Gef2 is a relatively stable protein on the cell cortex, similar to Mid1 (Celton-Morizur *et al.*, 2004; Zhang *et al.*, 2010; Laporte *et al.*, 2011). Consistently, Gef2 partially colocalized with Mid1 at interphase and cytokinesis nodes, as well as contractile ring before its constriction (Figure 5D). In addition, Gef2 also colocalized with Plo1 at the contractile ring during its formation, but no colocalization in nodes was detected (Figure 5D).

Then we examined how Gef2 is localized to the division site. In mammalian and *S. cerevisiae* cells, Polo kinases are crucial for the recruitment of Rho-GEF proteins to the division site (Yoshida *et al.*, 2006; Petronczki *et al.*, 2007, 2008). We tested whether Plo1 affected Gef2 localization. At 25°C, Gef2 localizations to nodes and the contractile ring were similar in *plo1-ts18* cells and wt cells (Figure 5E). After 2 h at 36°C, Gef2 still localized to the nodes in both wt and *plo1-ts18* mutant, although the signal decreased in *plo1-ts18* cells. Compared to the normal ring in wt, *plo1-ts18* cells, like *mid1Δ* cells, formed aberrant Gef2 ring or filamentous structures (Figure 5E). These results suggest that Plo1 is involved in but not required for Gef2 localization.

To determine the proteins required for Gef2 localization, we next examined the actin dependence of Gef2 localization (Figure 5F). In mitotic cells treated with latrunculin A (Lat-A), compared with cells in the dimethyl sulfoxide control, both Gef2 and Myo2 rings became discontinuous but remained at the division site. In addition, node localization of Gef2 was not affected. Similar results were obtained after 30-min treatment, indicating that Gef2 localization does not depend on actin filaments. Consistent with the results of Moseley *et al.* (2009), interphase nodes of Gef2 were abolished in *cdr2Δ* and *blt1Δ* cells (Figure 5G). Gef2 appeared in some scattered puncta in *cdr2Δ* cells and resembled Blt1 localization in *cdr2Δ* cells (Moseley *et al.*, 2009) but not in *blt1Δ* cells (Figure 5G), suggesting that Blt1 is required for Gef2 localization to interphase nodes. However, Gef2 still localized to cytokinesis nodes and the contractile ring in *cdr2Δ* and *blt1Δ* cells (Figure 5G). In *blt1Δ* cells, Gef2 cytokinesis nodes appeared 2.3 ± 1.8 min (n = 14 cells) after SPB separation (Figure 5H). Taken together, the results indicate that Gef2 localization depends on Blt1 during interphase but not during mitosis.

Gef2(957-1101) is sufficient for its localization, and the DBL-homology domain is important for division-site positioning

Gef2 is a putative Rho-GEF with 1101 amino acids (aa), which contains a conserved

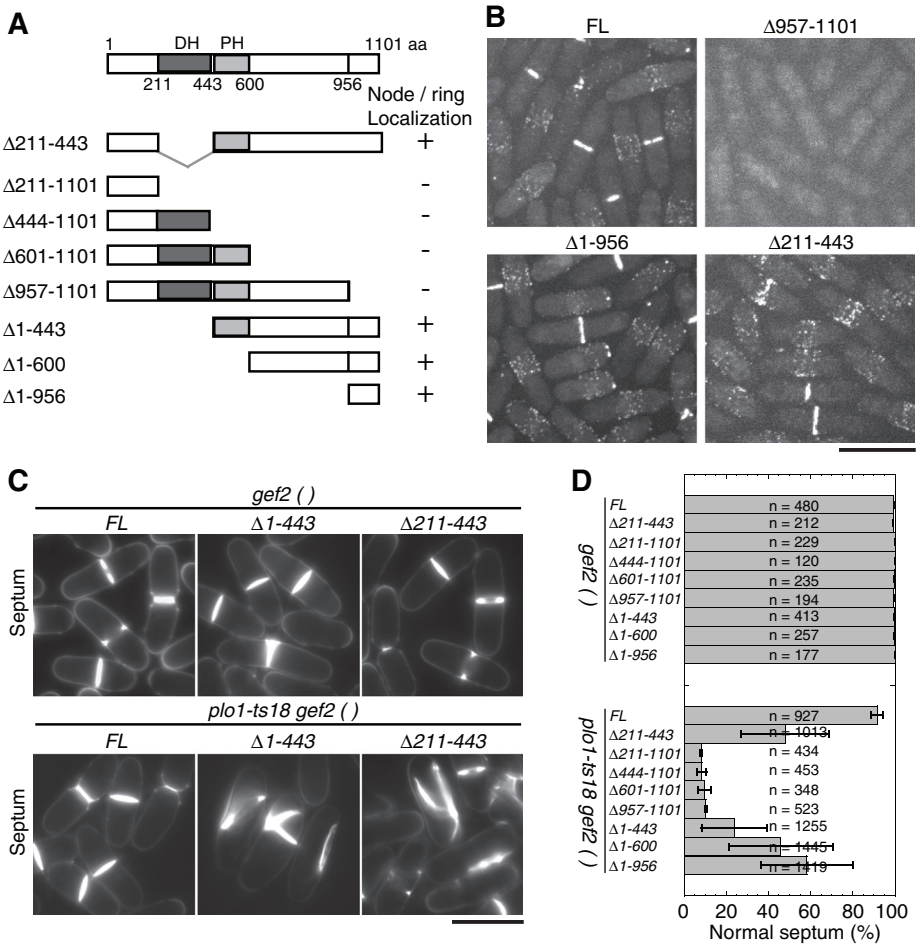

FIGURE 6: Importance of Gef2(957-1101) in Gef2 localization and the DH domain in division-site positioning. (A) Schematics of Gef2 domains and truncations constructed. For localization, a plus sign means that Gef2 localizes to nodes and the contractile ring, and a minus sign means no cortical localization. (B) Localizations of FL and truncated Gef2 in strains JW3825, JW4310, and JW3826, and JW3498. (C, D) Calcofluor staining of septa (C) and quantification of septum positioning (D) of *gef2* truncations and *gef2 plo1-ts18* mutants. Cells of JW3825, JW4238, JW4307-JW4310, JW3826-JW3828, JW3843, JW4241, JW4312-JW4315, and JW3856-3858 were grown at 25°C. Mean ± SD from two or three independent experiments is shown. Bars, 10 μm.

DBL-homology (DH) domain followed by a less conserved pleckstrin homology (PH) domain (Figure 6A). To dissect which region of Gef2 is required for its localization and function, we constructed Gef2 truncations under the native *gef2* promoter and integrated at the *gef2* locus (Figure 6A). We detected no Gef2 signals at cortical nodes or the contractile ring in the C-terminal truncations, even when only the last 145 aa were deleted, and the truncated Gef2 was diffused in the cells (Figure 6, A and B). Of interest, the last 145 aa were sufficient for localization to cortical nodes and the contractile ring (Figure 6B, Δ1-956). A weak nuclear signal was also detected in cells expressing Gef2(957-1101), (1-400), and (1-600) but not FL Gef2 (Figure 6B and unpublished data). On the other hand, the DH domain and other N-terminal regions were dispensable for Gef2 localization (Figure 6, A and B). Thus the C-terminal aa 957–1101 are required and sufficient for Gef2 localization.

We next tested how Gef2 domains/motifs contribute to Gef2 functions by crossing *gef2* truncations to *plo1-ts18* mutant (Figure 6, C and D). All the C-terminal truncations, which abolished the localization of Gef2 at nodes and the contractile ring, showed severe synthetic defects with the *plo1-ts18* mutant in septum positioning as *gef2Δ*. Even the smallest truncation, *gef2(Δ957-1101)*, showed 90 ± 0.4% abnormal septa in the *plo1-ts18* mutant. The double mutant of *gef2(Δ211-443) plo1-ts18* exhibited 52 ± 21% abnormal septum, indicating the DH domain is important for Gef2 function. The region upstream of the DH domain was also important since 76 ± 16% of the *gef2(Δ1-443) plo1-ts18* cells had abnormal septa. Of interest, the smallest fragment, Gef2(957-1101), which can localize to nodes and the contractile ring but lacks the DH domain, still possessed partial function in division-site positioning, since only 42 ± 22% of *gef2(Δ1-956) plo1-ts18* cells had abnormal septa. Together these results suggest that Gef2 localizations are important for its function in division-site positioning, and both the N-terminal aa 1-443, including the DH domain, and the C-terminus (601–1101) contribute to division-plane specification.

Gef2 is important for contractile-ring stability and disassembly during ring constriction

Besides the interactions with mutants involved in division-site positioning and contractile-ring assembly, we found that *gef2Δ* also showed genetic interactions with cytokinesis mutants involved in contractile-ring maturation and constriction. A synthetic defect was observed in *gef2Δ myp2Δ* double mutant. Myp2 is an unconventional myosin II, which localizes to the contractile ring during late anaphase B and is important for ring integrity and constriction (Bezanilla *et al.*, 1997, 2000). At 25°C, ~23% wt and *gef2Δ* cells contained one septum (Figure 7A). In *myp2Δ* mutant, although septating cells increased to 31%, septum morphology was mostly normal (Figure 7A). However, in *gef2Δ myp2Δ* mutant, 35% cells contained one septum, and 15% had more than one septum. Many of the septa were incomplete or aberrant, suggesting that Gef2 is involved in ring constriction or septum formation.

To further explore the defects in *gef2Δ myp2Δ* mutant, we used Rlc1-tandem Tomato (tdTomato) and GFP-Psy1 (Nakamura *et al.*, 2001) to examine the contractile ring and plasma membrane, respectively, during cytokinesis (Figure 7, B and C, and Supplemental Videos S8–S10). In wt and single-mutant cells, membrane invagination always occurred where a constricted ring was present. In some *myp2Δ* cells, asymmetric ring constriction was also observed (Figure 7, B and C, and Supplemental Videos S8 and S9). In contrast, the invaginated membrane and constricting ring were uncoupled in *gef2Δ myp2Δ* cells (Figure 7, B and C, and Supplemental Video S10). In time-lapse movies, we observed that membrane invagination was coupled with ring constriction at the beginning and then the ring drifted away, which caused a delay for membrane invagination and cell separation (Figure 7C). In some cases, the ring collapsed during constriction, and the cells immediately tried to reassemble another ring near the original division

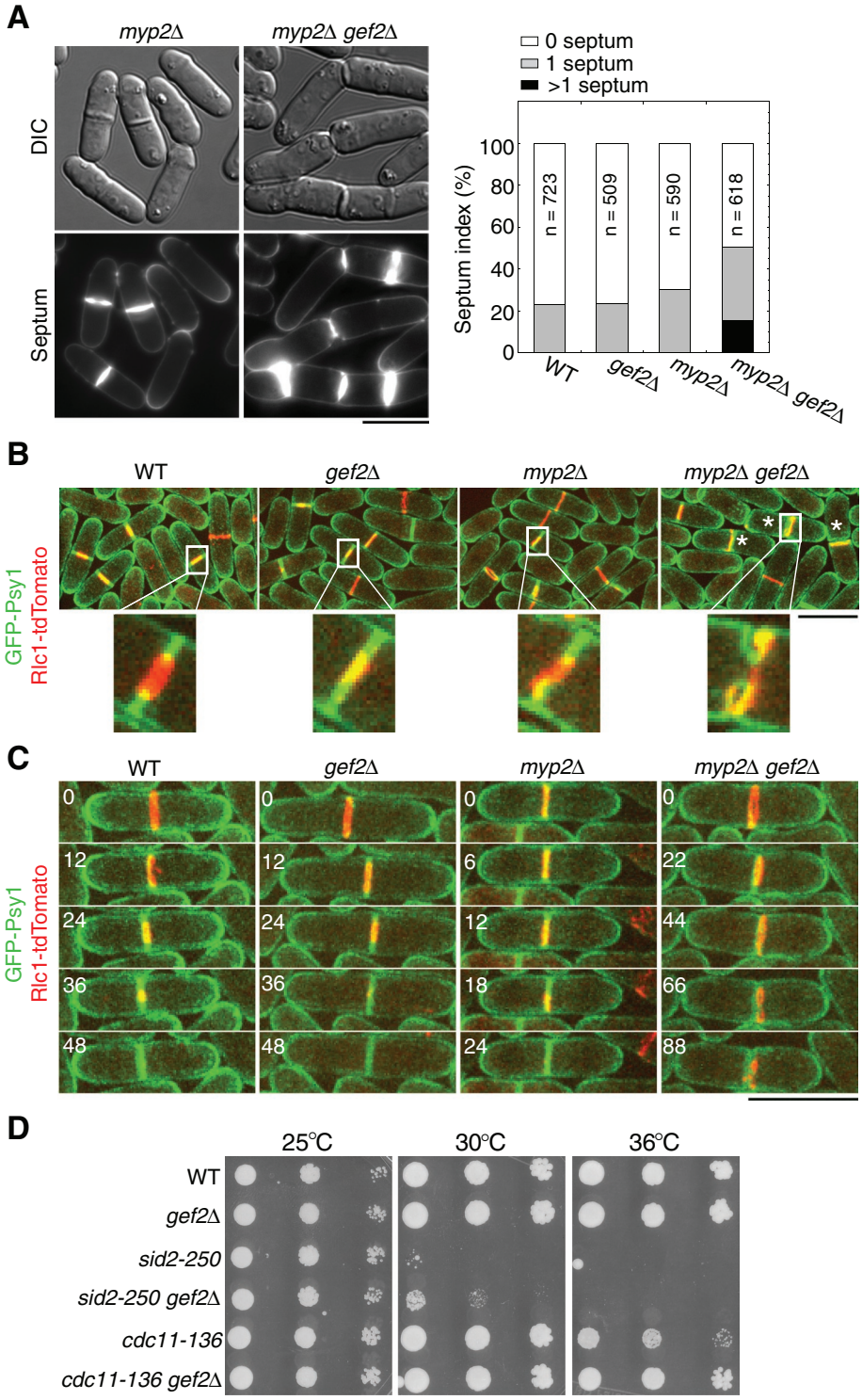

FIGURE 7: Gef2 is important for ring stability/anchoring during ring constriction. (A) DIC and septum staining of *myp2Δ* and *gef2Δ myp2Δ* mutants (left) and septation index of the indicated strains (right). JW729, JW1826, JW703, and JW2858 cells were grown in YE5S medium at 25°C for 36 h. (B, C) *gef2Δ myp2Δ* cells are defective in ring stability/anchoring and disassembly during ring constriction. Ring constriction and membrane invagination in JW3573, JW3574, JW2923, and JW2948 cells expressing GFP-Psy1 and Rlc1-tdTomato at 25°C. (B) Top, maximum-intensity projections of 12 z-projections at 0.5-μm spacing. Bottom, single focal plane of the magnified region within the white box. Asterisk indicates incomplete septa. (C) Time courses (in minutes) of ring constriction and membrane invagination. Images are maximum-intensity projections of eight z-projections at 0.75-μm spacing. Bars, 10 μm. (D) *gef2Δ* mutant suppresses SIN mutants *sid2-250* and *cdc11-136*. Strains JW739, JW3972, YDM429, JW3009, TP47, and JW2972 were grown in YE5S medium at 25°C. Cells (4×10^4) were serially diluted (10×) and grown on YE5S plate at 25, 30, and 36°C for 3 d.

site (Supplemental Video S10). Because the SIN pathway regulates ring disassembly (Krapp and Simanis, 2008; Roberts-Galbraith and Gould, 2008), we tested the genetic interactions between *gef2Δ* and SIN mutants. We found that *gef2Δ* mutant partially rescued the growth defects of SIN mutants *cdc11-136* and *sid2-250* at nonpermissive temperatures (Figure 7D). These results suggest that Gef2 plays a role in ring stability/anchoring and disassembly during late stages of cytokinesis.

DISCUSSION

Our data demonstrate that *S. pombe* putative Rho-GEF Gef2 is involved in division-site positioning and contractile-ring assembly through regulating Mid1 localization. In addition, Gef2 is also important for contractile-ring stability/anchoring and disassembly during ring constriction.

Gef2 and Plo1 coordinate for Mid1 localization and function

Mid1 phosphorylation by Polo kinase Plo1 triggers Mid1 nuclear export at the G2/M transition (Bähler *et al.*, 1998a; Almonacid *et al.*, 2011). Our data indicate that Gef2 helps Mid1 anchor to the plasma membrane through physical interactions with the Mid1 N-terminus. Then Mid1 serves as a scaffold for recruiting other proteins for contractile-ring assembly. Thus Gef2 and Plo1 coordinate and define new overlapping pathways for Mid1 localization and function.

Our results add another layer of complexity to Mid1 cortical targeting. Nuclear shuttling regulates the ratio between nuclear and cytoplasmic Mid1 (Bähler *et al.*, 1998a; Paoletti and Chang, 2000; Daga and Chang, 2005; Almonacid *et al.*, 2011). Two domains—Mid1(300-350) and Mid1(400-450)—have been identified to localize Mid1(1-506) to cortical nodes (Almonacid *et al.*, 2009). In addition, the C-terminal amphipathic helix plus the polybasic NLS domain (Celton-Morizur *et al.*, 2004) and the PH domain (Lee and Wu, 2012) are also important for Mid1 cortical targeting. Moreover, the cortical ER network limits Mid1's lateral diffusion on the membrane (Zhang *et al.*, 2010). The synthetic defects of *gef2Δ mid1* mutants also indicate that Mid1 localization and function are regulated by several pathways. Given the essential role of Mid1 in division-site selection, it is not surprising that fission yeast has several overlapping pathways to ensure the fidelity of Mid1 localization.

It is a common theme in animal cells that overlapping signals from central spindle and astral microtubules specify the cleavage site (Bringmann and Hyman, 2005;

Barr and Gruneberg, 2007; Cabernard *et al.*, 2010; Rankin and Wordeman, 2010). Although no evidence shows that Polo kinases phosphorylate anillins in multicellular organisms, anillins act synergistically with the centralspindlin complex for cleavage-furrow formation by interacting MgcRacGAP/RacGAP50C (Zhao and Fang, 2005; D'Avino *et al.*, 2008; Gregory *et al.*, 2008) and RhoA (Piekny and Glotzer, 2008). It will be interesting to explore whether anillins interact with Rho-GEF Ect2/Pebble in animal cells since it has been shown that Pebble controls anillin localization in *Drosophila* S2 cells (Hickson and O'Farrell, 2008). We do not know whether Mid1 binds to Gef2 directly or through a Rho GTPase. Moreover, it is unknown whether Gef2 is regulated by Polo kinase Plo1 through phosphorylation like other Rho-GEFs (Niiya *et al.*, 2006; Yoshida *et al.*, 2006). Nevertheless, our findings open new frontiers for studying division-site specification and contractile-ring assembly in both yeast and multicellular organisms.

The relationship between Gef2 and Cdr2 kinase in regulating Mid1 localization and function

Two overlapping mechanisms have been proposed to position Mid1 at the central cortex: one is the Cdr2-dependent anchoring of Mid1 in cortical nodes during interphase, and the other is Plo1-dependent Mid1 nuclear export at G2/M transition (Almonacid *et al.*, 2009). Now we find that Gef2 also plays overlapping functions with Plo1. What is the relationship between Gef2 and Cdr2 in regulating Mid1 localization to the central cortex?

First, *gef2Δ* has no obvious synthetic defects with *cdr2Δ* in division-site specification (Figure 2B), so they are not on overlapping pathways. Second, both Cdr2 and Gef2 interact with the Mid1 N-terminus, but this might be through different domains. Almonacid *et al.* (2009) shows that Cdr2 interacts with Mid1(400-450), and our results suggest that Gef2 likely binds to Mid1(300-350). The interaction between Gef2 and Mid1 is severely affected in the *mid1(Δ300-350)* strain (Figure 4G). The small amount of Mid1(Δ300-350) pulled down by Gef2 might be from indirect interactions through Blt1-Cdr2. We find that *mid1(Δ300-350) plo1-ts18* mimics *gef2Δ plo1-ts18* in septum-positioning defects, which is consistent with the proposed interaction between Gef2 and Mid1(300-350). Third, Cdr2 is more important than Gef2 for Mid1 localization during interphase. Mid1 is recruited to interphase nodes mainly by Cdr2 kinase, since Mid1 localization is dramatically reduced in *cdr2Δ* cells (Almonacid *et al.*, 2009; Moseley *et al.*, 2009) but is not obviously affected in *gef2Δ* (Figure 2, A–C). Gef2's role is more obvious for the localization of Mid1 N-terminus. Cortical nodes of Mid1 N-termini (1–580 or 1–506) are abolished in *gef2Δ*. Fourth, Gef2 is more important than Cdr2 for Mid1 localization and function during mitosis, based on several lines of evidence. The level of Cdr2 in cortical nodes decreases at early mitosis, and Cdr2 only transiently localizes to the contractile ring (Morrell *et al.*, 2004; Martin and Berthelot-Grosjean, 2009). In contrast, Gef2 remains in cytokinesis nodes and the contractile ring throughout cytokinesis. *gef2Δ plo1-ts18* cells have more severe defects in division-site positioning than *cdr2Δ plo1-ts18* and *blt1Δ plo1-ts18* cells, despite the lack of Gef2 localization to cortical nodes during interphase in *cdr2Δ* or *blt1Δ* cells. In addition, Mid1 N-terminal truncations localize to the contractile ring in *cdr2Δ* but not in *gef2Δ*. Furthermore, the Mid1-Cdr2 fusion protein localizes to interphase nodes normally but can only partially rescues the defect of *gef2Δ plo1-ts18* double mutant, indicating that the fusion protein cannot bypass the requirement for Gef2 during mitosis (Figure 3C).

Collectively, the results indicate that Cdr2 kinase and Gef2 have overlapping functions with Plo1 for Mid1 localization and division-site selection at different cell-cycle stages. Cdr2 is more important during interphase, and Gef2 is critical during mitosis. The overlapping mechanisms provide more precision and fidelity for cytokinesis. It will be interesting to know whether homologues of Cdr2 (Kishi *et al.*, 2005) and Gef2 in multicellular organisms play overlapping roles with Polo kinase in regulating anillin localizations and functions.

Gef2 localization and function

Gef2 localization is actin independent (Figure 5F). During interphase, Gef2 depends on both Cdr2 and Blt1 for localization to interphase nodes (Figure 5G; Moseley *et al.*, 2009). Because Blt1 localization depends on Cdr2 and Blt1 physically interacts with Gef2 (Moseley *et al.*, 2009), it is more likely that Blt1 directly recruits Gef2 to interphase nodes. Although Mid1 concentration in interphase nodes is not affected without Gef2, Mid1 becomes more dynamic (Figure 2, C and E), suggesting that Gef2 stabilizes Mid1 cortical localization during interphase. However, Cdr2 and Blt1 are not required for Gef2 localization to cytokinesis nodes and contractile ring during mitosis (Figure 5, G and H).

During mitosis, F-BAR protein Cdc15 might be involved in Gef2 localization. Gef2 appears in cytokinesis nodes ~2 min after SPB separation in *blt1Δ* cells (Figure 5H), which is after Cdc15 (Wu *et al.*, 2003; Laporte *et al.*, 2011). In addition, the Gef2 level in the contractile ring is dramatically reduced in *cdc15-140* cells at 36°C, and Cdc15 and Gef2 physically interact in IP (unpublished data). However, it is also possible that Gef2 binds to the plasma membrane directly using its last 145 aa, since this region is required for its localization (Figure 6, A and B). Consistently, Cdc15 is involved in the organization of lipid rafts (Takeda *et al.*, 2004). Cortical localization of human Ect2 requires a PH domain right downstream the DH domain and a polybasic cluster near its C-terminus (Chalamalasetty *et al.*, 2006; Su *et al.*, 2011). Of interest, Gef2 contains a domain with low similarity (16% identity and 43% similarity) to the PH domain of mouse Ect2, although it seems that this region is not important for Gef2 localization (Figure 6A). Thus further studies are needed to determine how Gef2 is localized during mitosis.

Budding yeast and mammalian Rho-GEFs such as Tus1 and Ect2 are known to regulate Rho1/RhoA activation by converting Rho from GDP-bound to GTP-bound status (Schmelzle *et al.*, 2002; Chalamalasetty *et al.*, 2006; Yoshida *et al.*, 2006). The DH domain of Gef2 is important for Gef2 function in division-site positioning (Figure 6). None of the six Rho GTPases has been shown to regulate Mid1 or localize to cortical nodes in fission yeast. Deletion mutants of *rho2 to rho5* showed no obvious defect in division-site positioning or contractile-ring assembly, even in the double mutants with *plo1-ts18* (unpublished data). Although Rgf3—a GEF for Rho1—might be involved in contractile-ring assembly (Mutoh *et al.*, 2005), the downstream effector(s) of Rho1 is unknown. Activated Cdc42 localizes to the contractile ring, and the localization depends on human BIN3 orthologue Hob3 (Merla and Johnson, 2000; Coll *et al.*, 2007). However, *hob3Δ* cells have defects in contractile-ring constriction but not formation (Coll *et al.*, 2007). Thus further studies are needed to investigate whether Gef2 has GEF activity and which Rho GTPase might be activated by Gef2.

Roles of Gef2 in contractile-ring stability and disassembly in late cytokinesis

Our data provide evidence that Gef2 plays a role in ring constriction during late cytokinesis. We find that Gef2 and Myp2 control contractile-ring stability/anchoring (Figure 7, B and C). In fission

yeast, the postanaphase array of microtubules is important for stabilizing the contractile ring (Pardo and Nurse, 2003), and Myp2 is important for its formation (Samejima *et al.*, 2010). However, *gef2Δ* showed no obvious genetic interactions with *mto1Δ* or *mto2Δ* mutants (unpublished data), which are also required for postanaphase array formation (Samejima *et al.*, 2005), suggesting that Gef2 and Myp2 regulate contractile-ring stability through a microtubule-independent pathway. Among the seven Rho GEFs, Rgf1–3 are also involved in late stages of cytokinesis (Tajadura *et al.*, 2004; Morrell-Falvey *et al.*, 2005; Mutoh *et al.*, 2005; Garcia *et al.*, 2006, 2009a, 2009b; Wu *et al.*, 2010). Our preliminary results show that Gef2 and Rgf1 have synthetic defects in cytokinesis. Further studies are needed to map out the redundancy among the Rho-GEFs in late stages of cytokinesis.

gef2Δ myp2Δ cells also have defects in contractile-ring disassembly (Supplemental Video S10), which suggests that the SIN pathway might be hyperactive or cannot be turned off in these cells (Krapp and Simanis, 2008; Roberts-Galbraith and Gould, 2008). Because *myp2Δ* is synthetic with SIN mutants *cdc11* and *cdc14* (Bezanilla *et al.*, 1997) but *gef2Δ* can partially suppress the growth defects of *sid2* and *cdc11* mutants (Figure 7D), Gef2 activity might be antagonistic to the SIN pathway during ring constriction. It will be interesting to determine the molecular mechanism of the suppression.

In conclusion, we find that the putative Rho-GEF Gef2 regulates division-site selection and contractile-ring assembly in fission yeast. Gef2 and Polo kinase coordinate to regulate the cortical localization of anillin Mid1. These findings provide the first evidence that Gef2 plays an important role in early steps of cytokinesis in fission yeast.

MATERIALS AND METHODS

Strains, genetics, molecular, and cellular methods

Strains used in this study are listed in Supplemental Table S1. Standard genetic and PCR-based gene targeting methods were used to transform yeast cells and construct strains (Moreno *et al.*, 1991; Bähler *et al.*, 1998b). All tagged, truncated, and fusion genes are under endogenous promoters and integrated into their native chromosomal loci, except for *Purg1-mid1* (under the control of *urg1* promoter and integrated at *mid1*$^+$ locus) and *leu1::Pmid1-mid1* (under *mid1* promoter and integrated at *leu1*$^+$ locus). The *urg1* promoter is induced when cells are grown in media with uracil (Watt *et al.*, 2008).

To construct *gef2* N-terminal truncations, *gef2* 5′ untranslated region (UTR; −600 to +3) was cloned into pFA6a-kanMX6-P3nmt1-mECitrine at *Bgl*II and *Pac*I sites. mECitrine was constructed from mYFP (S65G, V68L, Q69K, S72A, T203Y, and A206K) by introducing the F64L and Q69M mutations. The resulting plasmid was used as template, and *kanMX6-Pgef2-mECitrine* fragments were amplified by using primers corresponding to the desired truncations and transformed to wt strain as described (Bähler *et al.*, 1998b). The positive transformants were confirmed by PCR and/or sequencing.

To construct *gef2* C-terminal truncation strains, *ADH1* terminator with the selectable marker T_{ADH1}-*natMX6* or T_{ADH1}-*hphMX6* was amplified by PCR using primers corresponding to each truncation and transformed into mECitrine-*gef2* strain (JW3825) as described (Bähler *et al.*, 1998b). For constructing Gef2(Δ211-443)-mECitrine with the DH domain deleted (JW3498), a DNA fragment *gef2(631-3435)-mECitrine-natMX6* + 400 base pairs 3′ UTR of *gef2* was amplified by PCR from *gef2-mECitrine-natMX6* strain (JW2997) and cloned into the TOPO vector. Note that *gef2* has three introns. The resulting plasmid was used as template to amplify the DNA fragment *gef2(1330-3435)-mECitrine-natMX6* + 400 base pairs 3′ UTR of *gef2*, with the forward primer containing the first 70 base pairs, corresponding to *gef2*(561-630), and the last 20 base pairs corresponding to *gef2*(1330-1349), and the reverse primer (20 base pairs) complementary to the 3′ end of *gef2* 3′ UTR. Then the PCR fragment was transformed into the strain expressing Gef2(Δ211-1101)-mECitrine (JW3497). To construct Gef2(Δ211-443) without the C-terminal tag (JW4238), a DNA fragment *gef2(3132-3435)* + 442 base pairs 3′ UTR of *gef2* (*Tgef2*) was amplified by PCR and inserted into pFA6a-mYFP-kanMX6 at *Pac*I and *Bgl*II sites. The resulting plasmid was used as template to amplify *Tgef2-kanMX6* with the corresponding primers, and the PCR fragment was transformed into Gef2(Δ211-443)-mECitrine strain (JW3498). All truncations were confirmed by PCR and sequencing.

We tested the functionalities of tagged FL Gef2 in *plo1-ts18* background at 25°C. Approximately 50% of *gef2-mECitrine plo1-ts18* cells had abnormal septa, whereas only ~8% of *Pgef2-mECitrine-gef2 plo1-ts18* cells had abnormal septa, which is similar to *plo1-ts18* single mutant. Thus the N-terminally tagged Gef2 under its endogenous promoter is more functional than the C-terminally tagged one. However, for an unknown reason, both mECitrine-Gef2 and Gef2-mECitrine formed some aggregates at 36°C (Figure 5E). Thus tagged Gef2 may not be 100% functional.

To construct Mid1-Cdr2 fusion protein, *mid1-FL-linker* and *cdr2-mEGFP-kanMX6* were first cloned into the TOPO vector. *mid1-FL-linker* was amplified by using a forward primer starting 25 base pairs before the start codon of *mid1* ORF and a reverse primer complementary to the canonical C-terminal gene targeting linker CGGATCCCCGGGTTAATTAAC (Bähler *et al.*, 1998b). *Sal*I and *Pme*I sites were added to the reverse primer for further construction. *cdr2-mEGFP-kanMX6* was amplified from the genomic DNA of *cdr2-mEGFP* (JM346) using a forward primer with a *Sal*I site followed by the first 20 base pairs of *cdr2* and a reverse primer GAATTCGAGCTCGTTTAAAC. The reverse primer is complementary to the C-terminal–targeting module of pFA6a and has a *Pme*I site (Bähler *et al.*, 1998b). *cdr2-mEGFP-kanMX6* was then inserted into the 3′ end of *mid1-FL-linker* after *Sal*I and *Pme*I digestion and ligation. The resulting plasmid was digested by *Spe*I and *Xho*I. Then the fragment of *mid1-FL-linker-cdr2-mEGFP-kanMX6* was transformed into the strain *mid1-13Myc-hphMX6* (JW3206). The positive transformants were confirmed by PCR. The linker between Mid1 and Cdr2 is RIPGLINVD.

Septum staining with 10 μg/ml calcofluor and treatment with 100 μM Lat-A to depolymerize actin filaments were carried out as described (Wu *et al.*, 2001).

Microscopy and data analysis

Cells were restreaked from −80°C stocks, grown 1–2 d on yeast extract plus five supplements (YE5S) plates at 25°C, and then inoculated into 10-ml YE5S liquid cultures. Cells were grown at exponential phase for 18–48 h at 25°C except where noted. The short culture times for *gef2Δ plo1-ts18* were to prevent the effects of adaptation or second-site suppressor(s). Cells were collected from liquid cultures by centrifugation at 3500 rpm, washed with Edinburgh minimal medium plus five supplements (EMM5S), and resuspended in EMM5S with 0.1 mM *n*-propyl-gallate. Live-cell microscopy was carried out by loading samples onto a thin layer of 125 μl of EMM5S liquid medium with 20% gelatin (G-2500; Sigma-Aldrich, St. Louis, MO) and 0.1 mM *n*-propyl-gallate, sealed under a coverslip with valap, and observed at 23–25°C. Some samples were loaded directly onto slides for imaging at single time points.

For quantification of septation patterns, calcofluor-stained cells were imaged with a 100×/1.4 numerical aperture (NA) Plan-Apo objective lens on a Nikon Eclipse Ti inverted microscope (Nikon, Melville, NY) equipped with a Nikon cooled digital camera DS-QI1

and a 4′,6-diamidino-2-phenylindole (DAPI) filter. All other microscopy was carried out on a spinning disk confocal microscope (UltraVIEW ERS with CSU22 confocal head; PerkinElmer Life and Analytical Sciences, Waltham, MA) equipped with a 100×/1.4 NA Plan-Apo objective lens and an ORCA-AG camera (Hamamatsu, Hamamatsu, Japan) on a Nikon Eclipse TE2000-U inverted microscope. A 440-nm solid-state laser, 488- and 514-nm argon-ion lasers, and a 568-nm krypton-argon-ion laser were used for excitation.

Images were analyzed using ImageJ (Bethesda, MD) and UltraVIEW. Fluorescence images shown in figures and movies are maximum-intensity projections of stacks of images spanning whole cells at 0.4- or 0.5-µm spacing, except where noted otherwise. Fluorescence intensity was measured as described before (Coffman *et al.*, 2011; Laporte *et al.*, 2011). Briefly, 14 z-sections with 0.4-µm spacing were taken at the exactly same imaging conditions for all strains except the images used for mitotic Mid1 intensity measurement in *cdr2Δ* background, which were 12 z-sections with 0.5-µm spacing. The images were subtracted by the offset and corrected for the uneven illumination. Mean intensities in the whole cells were measured using sum intensity projections. The corresponding untagged strains were used for background subtraction. Mean intensities of interphase nodes were measured using a rectangular region of interest (ROI) with an average area of 60–85 pixels in the best focal plane. The intensities of the plasma membrane outside the ROI in the same cell were used for background subtraction (Figure 2C). Mid1 mean intensities in cytokinesis nodes and in the nucleus of early mitotic cells were measured using a rectangular or circular ROI with an average area of ~44 (for cytokinesis node) or ~328 (for nucleus) pixels in the best focal plane. The intensity of the cytoplasm outside the ROI in the same cell was used for background subtraction (Figure 2D). Because Mid1 signal spreads on the plasma membrane of *gef2Δ plo1-ts18* and *cdr2Δ gef2Δ plo1-ts18* cells during early mitosis, the smaller ROI and the cytoplasmic background (instead of the plasma membrane background) were used for the measurements. To count the Gef2 molecules, the global and local intensities of Gef2 and Mid1 were measured as described, and then the Gef2 intensities were normalized to Mid1 intensities to obtain molecule numbers (Wu and Pollard, 2005; Laporte *et al.*, 2011).

FRAP analysis

FRAP experiments were performed with the photokinesis unit on the UltraVIEW ERS confocal system as described (Coffman *et al.*, 2009; Laporte *et al.*, 2011). Optimal focal plane for bleaching was selected from z-sections. After collection of four prebleach images, the ROIs containing several cortical nodes were bleached >50% of the original signal, and 120 postbleach images with 10-s delay were collected. Intensity of every three consecutive time points was averaged to reduce noise. After subtracting the background and correcting for photobleaching during image acquisition (using intensity at unbleached region), the ROI intensity was normalized with the mean prebleach intensity set to 100% and the intensity just after bleaching set at 0%. Time 0 was set as first time point after bleaching. The exponential equation $y = m_1+m_2 \exp(-m_3x)$ was used for the curve fit, in which m_3 is the off-rate (KaleidaGraph; Synergy Software, Reading, PA). The half-time of recovery was calculated as $t_{1/2} = (\ln 2)/m_3$.

IP and Western blotting

Yeast cells expressing tagged proteins under the control of native promoters were harvested at exponential phase, washed with CXS buffer (50 mM 4-(2-hydroxyethyl)-1-piperazineethanesulfonic acid [HEPES], 20 mM KCl, 2 mM EDTA, 1 mM $MgCl_2$, pH 7.5), and frozen with liquid nitrogen in CXS buffer with EDTA-free protein inhibitor (Roche, Indianapolis, IN). A total of ~2×10^8 frozen cells were disrupted by grinding in mortar with liquid nitrogen. After thawing and centrifugation at 3500 rpm for 5 min at 4°C, lysis buffer (10 mM Tris, 130 mM NaCl, and 1% Triton, pH 8.0) was added to the crude extract, then centrifuged at 13,000 rpm for 20 min at 4°C. Thirty microliters of protein G covalently coupled magnetic Dynabeads (100.04D; Invitrogen, Carlsbad, CA) per sample was washed three times with cold phosphate-buffered saline (PBS) buffer (2.7 mM KCl, 137 mM NaCl, 10 mM Na_2HPO_4, and 2 mM KH_2PO_4, pH 7.4), and 5 µl of rabbit anti-YFP antibody (NB600-308; Novus Biologicals, Littleton, CO) per sample in PBS buffer was added to beads. After incubation for 1 h at room temperature, the beads were washed three times with PBS buffer and twice with CXS buffer. Cell extracts of ~200 µl were mixed with antibody-coupled Dynabeads and incubated for 1.5 h at 4°C. The precipitated beads were washed five times with CXS buffer plus 1% Triton, then dissolved in sample buffer and boiled for 5 min. After separation of proteins in SDS–PAGE, Western blotting was performed as described (Laporte *et al.*, 2011) using monoclonal anti–GFP/YFP JL-8 antibody (632381, 1:2500 dilution; Clontech,) or monoclonal anti-Myc antibody (9E10, 1:2500 dilution; Santa Cruz Biotechnology, Santa Cruz, CA).

For Mid1 total protein analysis (Supplemental Figure S2), yeast cells were harvested at exponential phase, washed twice with double-distilled H_2O, and resuspended in LiAc/SDS buffer (200 mM LiAc, 1% SDS, pH 7.5). After incubation at 65°C for 10 min, cells were mixed with sample buffer and boiled for 5 min. After centrifugation at 3000 rpm for 5 min, proteins in the supernatant were separated in SDS–PAGE, and Western blotting was performed as described. The intensities of Mid1 and tubulin bands were measured using Image J. The intensity for each strain was subtracted by the background of the same size in a nearby area before ratio comparison.

ACKNOWLEDGMENTS

We thank Anne Paoletti, Iain Hagan, Dannel McCollum, Jürg Bähler, John Pringle, James Moseley, Paul Nurse, Fred Chang, Taro Nakamura, and the Yeast Genetic Resource Center Japan (supported by the National BioResource Project) for strains. We thank members of the Wu laboratory for helpful discussions and suggestions. This work was partially supported by a Basil O'Connor Starter Scholar Research Award to J.-Q.W. and National Institutes of Health Grants R01AG19960 to K.W.R. and R01GM086546 to J.-Q.W.

REFERENCES

Almonacid M, Celton-Morizur S, Jakubowski JL, Dingli F, Loew D, Mayeux A, Chen JS, Gould KL, Clifford DM, Paoletti A (2011). Temporal control of contractile ring assembly by Plo1 regulation of myosin II recruitment by Mid1/anillin. Curr Biol 21, 473–479.

Almonacid M, Moseley JB, Janvore J, Mayeux A, Fraisier V, Nurse P, Paoletti A (2009). Spatial control of cytokinesis by Cdr2 kinase and Mid1/anillin nuclear export. Curr Biol 19, 961–966.

Almonacid M, Paoletti A (2010). Mechanisms controlling division-plane positioning. Semin Cell Dev Biol 21, 874–880.

Bähler J, Steever AB, Wheatley S, Wang Y-l, Pringle JR, Gould KL, McCollum D (1998a). Role of Polo kinase and Mid1p in determining the site of cell division in fission yeast. J Cell Biol 143, 1603–1616.

Bähler J, Wu J-Q, Longtine MS, Shah NG, McKenzie A, III, Steever AB, Wach A, Philippsen P, Pringle JR (1998b). Heterologous modules for efficient and versatile PCR-based gene targeting in *Schizosaccharomyces pombe*. Yeast 14, 943–951.

Balasubramanian MK, Bi E, Glotzer M (2004). Comparative analysis of cytokinesis in budding yeast, fission yeast and animal cells. Curr Biol 14, R806–R818.

Barr FA, Gruneberg U (2007). Cytokinesis: placing and making the final cut. Cell 131, 847–860.

Bezanilla M, Forsburg SL, Pollard TD (1997). Identification of a second myosin-II in *Schizosaccharomyces pombe*: Myp2p is conditionally required for cytokinesis. Mol Biol Cell 8, 2693–2705.
Bezanilla M, Wilson JM, Pollard TD (2000). Fission yeast myosin-II isoforms assemble into contractile rings at distinct times during mitosis. Curr Biol 10, 397–400.
Breeding CS, Hudson J, Balasubramanian MK, Hemmingsen SM, Young PG, Gould KL (1998). The *cdr2*$^+$ gene encodes a regulator of G2/M progression and cytokinesis in *Schizosaccharomyces pombe*. Mol Biol Cell 9, 3399–3415.
Bringmann H, Hyman AA (2005). A cytokinesis furrow is positioned by two consecutive signals. Nature 436, 731–734.
Cabernard C, Prehoda KE, Doe CQ (2010). A spindle-independent cleavage furrow positioning pathway. Nature 467, 91–94.
Calonge TM, Nakano K, Arellano M, Arai R, Katayama S, Toda T, Mabuchi I, Perez P (2000). *Schizosaccharomyces pombe* Rho2p GTPase regulates cell wall α-glucan biosynthesis through the protein kinase Pck2p. Mol Biol Cell 11, 4393–4401.
Celton-Morizur S, Bordes N, Fraisier V, Tran PT, Paoletti A (2004). C-terminal anchoring of mid1p to membranes stabilizes cytokinetic ring position in early mitosis in fission yeast. Mol Cell Biol 24, 10621–10635.
Celton-Morizur S, Racine V, Sibarita JB, Paoletti A (2006). Pom1 kinase links division plane position to cell polarity by regulating Mid1p cortical distribution. J Cell Sci 119, 4710–4718.
Chalamalasetty RB, Hummer S, Nigg EA, Sillje HH (2006). Influence of human Ect2 depletion and overexpression on cleavage furrow formation and abscission. J Cell Sci 119, 3008–3019.
Chang F, Wollard A, Nurse P (1996). Isolation and characterization of fission yeast mutants defective in the assembly and placement of the contractile actin ring. J Cell Sci 109, 131–142.
Coffman VC, Nile AH, Lee I-J, Liu H, Wu J-Q (2009). Roles of formin nodes and myosin motor activity in Mid1p-dependent contractile-ring assembly during fission yeast cytokinesis. Mol Biol Cell 20, 5195–5210.
Coffman VC, Wu P, Parthun MR, Wu J-Q (2011). CENP-A exceeds microtubule attachment sites in centromere clusters of both budding and fission yeast. J Cell Biol 195, 563–572.
Coll PM, Rincon SA, Izquierdo RA, Perez P (2007). Hob3p, the fission yeast ortholog of human BIN3, localizes Cdc42p to the division site and regulates cytokinesis. EMBO J 26, 1865–1877.
Coll PM, Trillo Y, Ametzazurra A, Perez P (2003). Gef1p, a new guanine nucleotide exchange factor for Cdc42p, regulates polarity in *Schizosaccharomyces pombe*. Mol Biol Cell 14, 313–323.
D'Avino PP, Takeda T, Capalbo L, Zhang W, Lilley KS, Laue ED, Glover DM (2008). Interaction between anillin and RacGAP50C connects the actomyosin contractile ring with spindle microtubules at the cell division site. J Cell Sci 121, 1151–1158.
Daga RR, Chang F (2005). Dynamic positioning of the fission yeast cell division plane. Proc Natl Acad Sci USA 102, 8228–8232.
Fujiwara T, Bandi M, Nitta M, Ivanova EV, Bronson RT, Pellman D (2005). Cytokinesis failure generating tetraploids promotes tumorigenesis in *p53*-null cells. Nature 437, 1043–1047.
Garcia P, Garcia I, Marcos F, de Garibay GR, Sanchez Y (2009a). Fission yeast Rgf2p is a Rho1p guanine nucleotide exchange factor required for spore wall maturation and for the maintenance of cell integrity in the absence of Rgf1p. Genetics 181, 1321–1334.
Garcia P, Tajadura V, Garcia I, Sanchez Y (2006). Rgf1p is a specific Rho1-GEF that coordinates cell polarization with cell wall biogenesis in fission yeast. Mol Biol Cell 17, 1620–1631.
Garcia P, Tajadura V, Sanchez Y (2009b). The Rho1p exchange factor Rgf1p signals upstream from the Pmk1 mitogen-activated protein kinase pathway in fission yeast. Mol Biol Cell 20, 721–731.
Gregory SL, Ebrahimi S, Milverton J, Jones WM, Bejsovec A, Saint R (2008). Cell division requires a direct link between microtubule-bound RacGAP and anillin in the contractile ring. Curr Biol 18, 25–29.
Hachet O, Berthelot-Grosjean M, Kokkoris K, Vincenzetti V, Moosbrugger J, Martin SG (2011). A phosphorylation cycle shapes gradients of the DYRK family kinase Pom1 at the plasma membrane. Cell 145, 1116–1128.
Hachet O, Simanis V (2008). Mid1p/anillin and the septation initiation network orchestrate contractile ring assembly for cytokinesis. Genes Dev 22, 3205–3216.
Hall A (1998). Rho GTPases and the actin cytoskeleton. Science 279, 509–514.
Hickson GR, O'Farrell PH (2008). Rho-dependent control of anillin behavior during cytokinesis. J Cell Biol 180, 285–294.
Hiraoka Y, Toda T, Yanagida M (1984). The *NDA3* gene of fission yeast encodes β-tubulin: a cold-sensitive *nda3* mutation reversibly blocks spindle formation and chromosome movement in mitosis. Cell 39, 349–358.
Hirota K, Tanaka K, Ohta K, Yamamoto M (2003). Gef1p and Scd1p, the two GDP-GTP exchange factors for Cdc42p, form a ring structure that shrinks during cytokinesis in *Schizosaccharomyces pombe*. Mol Biol Cell 14, 3617–3627.
Huang Y, Chew TG, Ge W, Balasubramanian MK (2007). Polarity determinants Tea1p, Tea4p, and Pom1p inhibit division-septum assembly at cell ends in fission yeast. Dev Cell 12, 987–996.
Huang Y, Yan H, Balasubramanian MK (2008). Assembly of normal actomyosin rings in the absence of Mid1p and cortical nodes in fission yeast. J Cell Biol 183, 979–988.
Iwaki N, Karatsu K, Miyamoto M (2003). Role of guanine nucleotide exchange factors for Rho family GTPases in the regulation of cell morphology and actin cytoskeleton in fission yeast. Biochem Biophys Res Commun 312, 414–420.
Karagiannis J, Bimbo A, Rajagopalan S, Liu J, Balasubramanian MK (2005). The nuclear kinase Lsk1p positively regulates the septation initiation network and promotes the successful completion of cytokinesis in response to perturbation of the actomyosin ring in *Schizosaccharomyces pombe*. Mol Biol Cell 16, 358–371.
Kishi M, Pan YA, Crump JG, Sanes JR (2005). Mammalian SAD kinases are required for neuronal polarization. Science 307, 929–932.
Kovar DR, Kuhn JR, Tichy AL, Pollard TD (2003). The fission yeast cytokinesis formin Cdc12p is a barbed end actin filament capping protein gated by profilin. J Cell Biol 161, 875–887.
Krapp A, Simanis V (2008). An overview of the fission yeast septation initiation network (SIN). Biochem Soc Trans 36, 411–415.
Laporte D, Coffman VC, Lee I-J, Wu J-Q (2011). Assembly and architecture of precursor nodes during fission yeast cytokinesis. J Cell Biol 192, 1005–1021.
Laporte D, Zhao R, Wu J-Q (2010). Mechanisms of contractile-ring assembly in fission yeast and beyond. Semin Cell Dev Biol 21, 892–898.
Lee I-J, Wu J-Q (2012). Characterization of Mid1 domains for targeting and scaffolding in fission yeast cytokinesis. J Cell Sci (*in press*).
MacIver FH, Glover DM, Hagan IM (2003). A "marker switch" approach for targeted mutagenesis of genes in *Schizosaccharomyces pombe*. Yeast 20, 587–594.
Martin SG, Berthelot-Grosjean M (2009). Polar gradients of the DYRK-family kinase Pom1 couple cell length with the cell cycle. Nature 459, 852–856.
Martin SG, Chang F (2006). Dynamics of the formin for3p in actin cable assembly. Curr Biol 16, 1161–1170.
Merla A, Johnson DI (2000). The Cdc42p GTPase is targeted to the site of cell division in the fission yeast *Schizosaccharomyces pombe*. Eur J Cell Biol 79, 469–477.
Moreno S, Klar A, Nurse P (1991). Molecular genetic analysis of fission yeast *Schizosaccharomyces pombe*. Methods Enzymol 194, 795–823.
Morrell JL, Nichols CB, Gould KL (2004). The GIN4 family kinase, Cdr2p, acts independently of septins in fission yeast. J Cell Sci 117, 5293–5302.
Morrell-Falvey JL, Ren L, Feoktistova A, Haese GD, Gould KL (2005). Cell wall remodeling at the fission yeast cell division site requires the Rho-GEF Rgf3p. J Cell Sci 118, 5563–5573.
Moseley JB, Mayeux A, Paoletti A, Nurse P (2009). A spatial gradient coordinates cell size and mitotic entry in fission yeast. Nature 459, 857–860.
Mutoh T, Nakano K, Mabuchi I (2005). Rho1-GEFs Rgf1 and Rgf2 are involved in formation of cell wall and septum, while Rgf3 is involved in cytokinesis in fission yeast. Genes Cells 10, 1189–1202.
Nakamura T, Nakamura-Kubo M, Hirata A, Shimoda C (2001). The *Schizosaccharomyces pombe spo3*$^+$ gene is required for assembly of the forespore membrane and genetically interacts with *psy1*$^+$-encoding syntaxin-like protein. Mol Biol Cell 12, 3955–3972.
Nakano K, Arai R, Mabuchi I (2005). Small GTPase Rho5 is a functional homologue of Rho1, which controls cell shape and septation in fission yeast. FEBS Lett 579, 5181–5186.
Nakano K, Imai J, Arai R, Toh EA, Matsui Y, Mabuchi I (2002). The small GTPase Rho3 and the diaphanous/formin For3 function in polarized cell growth in fission yeast. J Cell Sci 115, 4629–4639.
Niiya F, Tatsumoto T, Lee KS, Miki T (2006). Phosphorylation of the cytokinesis regulator ECT2 at G2/M phase stimulates association of the mitotic kinase Plk1 and accumulation of GTP-bound RhoA. Oncogene 25, 827–837.
Nishimura Y, Yonemura S (2006). Centralspindlin regulates ECT2 and RhoA accumulation at the equatorial cortex during cytokinesis. J Cell Sci 119, 104–114.

Ojkic N, Wu J-Q, Vavylonis D (2011). Model of myosin node aggregation into a contractile ring: the effect of local alignment. J Phys Condens Matter 23, 374103.
Padmanabhan A, Bakka K, Sevugan M, Naqvi NI, D'Souza V, Tang X, Mishra M, Balasubramanian MK (2011). IQGAP-related Rng2p organizes cortical nodes and ensures position of cell division in fission yeast. Curr Biol 21, 467–472.
Padte NN, Martin SG, Howard M, Chang F (2006). The cell-end factor Pom1p inhibits Mid1p in specification of the cell division plane in fission yeast. Curr Biol 16, 2480–2487.
Paoletti A, Chang F (2000). Analysis of mid1p, a protein required for placement of the cell division site, reveals a link between the nucleus and the cell surface in fission yeast. Mol Biol Cell 11, 2757–2773.
Pardo M, Nurse P (2003). Equatorial retention of the contractile actin ring by microtubules during cytokinesis. Science 300, 1569–1574.
Petronczki M, Glotzer M, Kraut N, Peters JM (2007). Polo-like kinase 1 triggers the initiation of cytokinesis in human cells by promoting recruitment of the RhoGEF Ect2 to the central spindle. Dev Cell 12, 713–725.
Petronczki M, Lenart P, Peters JM (2008). Polo on the rise-from mitotic entry to cytokinesis with Plk1. Dev Cell 14, 646–659.
Piekny AJ, Glotzer M (2008). Anillin is a scaffold protein that links RhoA, actin, and myosin during cytokinesis. Curr Biol 18, 30–36.
Piekny AJ, Maddox AS (2010). The myriad roles of anillin during cytokinesis. Semin Cell Dev Biol 21, 881–891.
Pollard TD, Wu J-Q (2010). Understanding cytokinesis: lessons from fission yeast. Nat Rev Mol Cell Biol 11, 149–155.
Rankin KE, Wordeman L (2010). Long astral microtubules uncouple mitotic spindles from the cytokinetic furrow. J Cell Biol 190, 35–43.
Roberts-Galbraith RH, Gould KL (2008). Stepping into the ring: the SIN takes on contractile ring assembly. Genes Dev 22, 3082–3088.
Sagona AP, Stenmark H (2010). Cytokinesis and cancer. FEBS Lett 584, 2652–2661.
Samejima I, Lourenco PC, Snaith HA, Sawin KE (2005). Fission yeast mto2p regulates microtubule nucleation by the centrosomin-related protein mto1p. Mol Biol Cell 16, 3040–3051.
Samejima I, Miller VJ, Rincon SA, Sawin KE (2010). Fission yeast Mto1 regulates diversity of cytoplasmic microtubule organizing centers. Curr Biol 20, 1959–1965.
Santos B, Martin-Cuadrado AB, Vazquez de Aldana CR, del Rey F, Perez P (2005). Rho4 GTPase is involved in secretion of glucanases during fission yeast cytokinesis. Eukaryot Cell 4, 1639–1645.
Sato M, Toya M, Toda T (2009). Visualization of fluorescence-tagged proteins in fission yeast: the analysis of mitotic spindle dynamics using GFP-tubulin under the native promoter. Methods Mol Biol 545, 185–203.
Schmelzle T, Helliwell SB, Hall MN (2002). Yeast protein kinases and the RHO1 exchange factor TUS1 are novel components of the cell integrity pathway in yeast. Mol Cell Biol 22, 1329–1339.
Shandala T, Gregory SL, Dalton HE, Smallhorn M, Saint R (2004). Citron kinase is an essential effector of the Pbl-activated Rho signalling pathway in *Drosophila melanogaster*. Development 131, 5053–5063.
Sohrmann M, Fankhauser C, Brodbeck C, Simanis V (1996). The *dmf1/mid1* gene is essential for correct positioning of the division septum in fission yeast. Genes Dev 10, 2707–2719.
Somers WG, Saint R (2003). A RhoGEF and Rho family GTPase-activating protein complex links the contractile ring to cortical microtubules at the onset of cytokinesis. Dev Cell 4, 29–39.
Storchova Z, Pellman D (2004). From polyploidy to aneuploidy, genome instability and cancer. Nat Rev Mol Cell Biol 5, 45–54.
Su KC, Takaki T, Petronczki M (2011). Targeting of the RhoGEF Ect2 to the equatorial membrane controls cleavage furrow formation during cytokinesis. Dev Cell 21, 1104–1115.
Tajadura V, Garcia B, Garcia I, Garcia P, Sanchez Y (2004). *Schizosaccharomyces pombe* Rgf3p is a specific Rho1 GEF that regulates cell wall beta-glucan biosynthesis through the GTPase Rho1p. J Cell Sci 117, 6163–6174.
Takeda T, Kawate T, Chang F (2004). Organization of a sterol-rich membrane domain by cdc15p during cytokinesis in fission yeast. Nat Cell Biol 6, 1142–1144.
Tolliday N, VerPlank L, Li R (2002). Rho1 directs formin-mediated actin ring assembly during budding yeast cytokinesis. Curr Biol 12, 1864–1870.
Vavylonis D, Wu J-Q, Hao S, O'Shaughnessy B, Pollard TD (2008). Assembly mechanism of the contractile ring for cytokinesis by fission yeast. Science 319, 97–100.
Wachtler V, Rajagopalan S, Balasubramanian MK (2003). Sterol-rich plasma membrane domains in the fission yeast *Schizosaccharomyces pombe*. J Cell Sci 116, 867–874.
Wang H, Tang X, Balasubramanian MK (2003). Rho3p regulates cell separation by modulating exocyst function in *Schizosaccharomyces pombe*. Genetics 164, 1323–1331.
Watt S, Mata J, Lopez-Maury L, Marguerat S, Burns G, Bähler J (2008). *urg1*: a uracil-regulatable promoter system for fission yeast with short induction and repression times. PLoS ONE 3, e1428.
Wolfe BA, Takaki T, Petronczki M, Glotzer M (2009). Polo-like kinase 1 directs assembly of the HsCyk-4 RhoGAP/Ect2 RhoGEF complex to initiate cleavage furrow formation. PLoS Biol 7, e1000110.
Wu J-Q, Bähler J, Pringle JR (2001). Roles of a fimbrin and an alpha-actinin-like protein in fission yeast cell polarization and cytokinesis. Mol Biol Cell 12, 1061–1077.
Wu J-Q, Kuhn JR, Kovar DR, Pollard TD (2003). Spatial and temporal pathway for assembly and constriction of the contractile ring in fission yeast cytokinesis. Dev Cell 5, 723–734.
Wu J-Q, Pollard TD (2005). Counting cytokinesis proteins globally and locally in fission yeast. Science 310, 310–314.
Wu J-Q, Sirotkin V, Kovar DR, Lord M, Beltzner CC, Kuhn JR, Pollard TD (2006). Assembly of the cytokinetic contractile ring from a broad band of nodes in fission yeast. J Cell Biol 174, 391–402.
Wu J-Q, Ye Y, Wang N, Pollard TD, Pringle JR (2010). Cooperation between the septins and the actomyosin ring and role of a cell-integrity pathway during cell division in fission yeast. Genetics 186, 897–915.
Yoshida S, Kono K, Lowery DM, Bartolini S, Yaffe MB, Ohya Y, Pellman D (2006). Polo-like kinase Cdc5 controls the local activation of Rho1 to promote cytokinesis. Science 313, 108–111.
Yüce Ö, Piekny A, Glotzer M (2005). An ECT2-centralspindlin complex regulates the localization and function of RhoA. J Cell Biol 170, 571–582.
Zhang D, Vjestica A, Oliferenko S (2010). The cortical ER network limits the permissive zone for actomyosin ring assembly. Curr Biol 20, 1029–1034.
Zhao WM, Fang G (2005). MgcRacGAP controls the assembly of the contractile ring and the initiation of cytokinesis. Proc Natl Acad Sci USA 102, 13158–13163.